

Precision nuclear structure in the in-medium similarity renormalization group

Matthias Heinz

April 14, 2020

Erklärung zur Abschlussarbeit gemäß § 22 Abs. 7 und § 23 Abs. 7 APB TU Darmstadt

Hiermit versichere ich, Matthias Heinz, das vorliegende Projekt-Proposal gemäß § 22 Abs. 7 APB der TU Darmstadt ohne Hilfe Dritter und nur mit den angegebenen Quellen und Hilfsmitteln angefertigt zu haben. Alle Stellen, die Quellen entnommen wurden, sind als solche kenntlich gemacht worden. Diese Arbeit hat in gleicher oder ähnlicher Form noch keiner Prüfungsbehörde vorgelegen.

Mir ist bekannt, dass im Falle eines Plagiats (§ 38 Abs. 2 APB) ein Täuschungsversuch vorliegt, der dazu führt, dass die Arbeit mit 5,0 bewertet und damit ein Prüfungsversuch verbraucht wird. Abschlussarbeiten dürfen nur einmal wiederholt werden.

Bei der abgegebenen Thesis stimmen die schriftliche und die zur Archivierung eingereichte elektronische Fassung gemäß § 23 Abs. 7 APB überein.

English translation for information purposes only:

Thesis statement pursuant to § 22 paragraph 7 and § 23 paragraph 7 of APB TU Darmstadt

I herewith formally declare that I, Matthias Heinz, have written the submitted thesis proposal independently pursuant to § 22 paragraph 7 of APB TU Darmstadt. I did not use any outside support except for the quoted literature and other sources mentioned in the paper. I clearly marked and separately listed all of the literature and all of the other sources which I employed when producing this academic work, either literally or in content. This thesis has not been handed in or published before in the same or similar form.

I am aware, that in case of an attempt at deception based on plagiarism (§ 38 paragraph 2 APB), the thesis would be graded with 5,0 and counted as one failed examination attempt. The thesis may only be repeated once.

In the submitted thesis the written copies and the electronic version for archiving are pursuant to § 23 paragraph 7 of APB identical in content.

Darmstadt, den 14. April 2020

(Matthias Heinz)

Abstract

The in-medium similarity renormalization group (IM-SRG) is an *ab initio* many-body method used to great success to model medium-mass nuclear systems. Its computational cost scales polynomially, and its formalism is highly flexible, leading to multiple variants that have been developed to extend its original closed-shell formulation to open-shell systems.

The current state-of-the-art implementations truncate the IM-SRG equations at the normal-ordered two-body level, the first non-trivial order in the expansion. In this work, we seek to systematically study the effects of extending this truncation to the normal-ordered three-body level, the so-called IM-SRG(3). We present the results of the current implementation for ${}^4\text{He}$ and the pairing Hamiltonian, calculations done to validate our implementation against previous calculations. We also discuss the steps still to be taken to arrive at an implementation that will allow for a careful study of the effects of the IM-SRG(3) truncation for nuclear systems.

Contents

Contents	vii
List of Figures	ix
1 Introduction	1
1.1 Goals	3
1.2 Outline	4
2 Nuclear forces	5
2.1 Nuclear forces from chiral effective field theory	5
2.2 Similarity renormalization group evolution of nuclear forces	8
2.3 Representations of nuclear potentials	10
2.3.1 Jacobi momentum space	11
2.3.2 Jacobi harmonic-oscillator space	12
2.3.3 Single-particle harmonic-oscillator space	13
3 Many-body basics and wave function expansion methods	15
3.1 Second quantization	15
3.2 Normal ordering	18
3.2.1 General properties	18
3.2.2 Vacuum normal ordering	19
3.2.3 In-medium normal ordering	20
3.3 The Hartree-Fock method	23
3.4 Many-body perturbation theory	24
3.5 Non-perturbative techniques	28
4 The in-medium similarity renormalization group	31
4.1 Basic formalism	31
4.2 Truncation schemes	33
4.2.1 IM-SRG(2)	34
4.2.2 IM-SRG(3)	35
4.3 Generator selection	37
4.4 The Magnus expansion	41

5	Results	45
5.1	The pairing Hamiltonian	45
5.2	${}^4\text{He}$	47
6	Summary and outlook	51
	Bibliography	53

List of Figures

1.1	The nuclear landscape, with stable and unstable atomic nuclei denoted by the black and green squares, respectively, and a theoretical prediction of the limit of bound nuclei being indicated by the red bands.	2
1.2	Chart of nuclides showing in red nuclei for which <i>ab initio</i> calculations involving two- and three-body interactions had been done in 2009 (top left) to 2018 (bottom right). Only calculations for which convergence with respect to basis size was achieved are included in the charts.	3
2.1	The contributions to NN, 3N, and 4N interactions in chiral EFT up to order N4LO. Solid lines indicate nucleon propagators. Dashed lines indicate pion propagators. The number of new LECs for the new interaction contributions at each new order is shown in the top right corner.	6
2.2	The total proton-neutron scattering cross section calculated order by order at different energies using chiral potentials with 68% and 95% degree of belief intervals indicated by the thick and thin error bars obtained via Bayesian uncertainty quantification.	8
2.3	An example of an SRG-evolved potential using the chiral EMN NN potential at N4LO in the 3S_1 part of the 3S_1 - 3D_1 channel.	10
3.1	The partial sums (left) and order-by-order contributions (right) for an MBPT calculation of the ground-state energy of ^{16}O using a harmonic-oscillator reference state (top) and a Hartree-Fock reference state (bottom). The red, blue, and yellow points are for $N_{\text{max}} = 2, 4$, and 6 , the basis truncation parameter for the approach used.	27
4.1	Schematic diagram showing the minimal decoupling scheme taken in the IM-SRG.	37
5.1	The correlation energy E_{corr} for the solution of the pairing Hamiltonian obtained via exact diagonalization, IM-SRG(2), and IM-SRG(3) for $-1 \leq g \leq 1$	46

- 5.2 The left panel shows $E(0)$ and $E(\infty)$ for an IM-SRG(2) calculation of ${}^4\text{He}$ for $\hbar\Omega$ ranging from 16 MeV to 32 MeV. The interaction used is the EM NN interaction with a regulator cutoff $\Lambda = 500$ MeV and SRG-evolved to $\lambda = 1.8\text{ fm}^{-1}$. The right panel shows the flowing energy $E(s)$ along with the energy with second- and third-order MBPT corrections included for $\hbar\Omega = 32$ MeV. . 48

Chapter 1

Introduction

Nuclear physics aims to understand systems where the structure and dynamics are dominated by the strong interaction, one of the four fundamental forces of nature. The goals of nuclear science are well-described by the overarching open questions identified by the U.S. National Academy of Science in *Exploring the Heart of Matter* [1]:

1. How did matter come into being and how does it evolve?
2. How does subatomic matter organize itself and what phenomena emerge?
3. Are the fundamental interactions that are basic to the structure of matter fully understood?
4. How can the knowledge and technological progress provided by nuclear physics best be used to benefit society?

At the heart of this work is the second question, with the focus of our attention being on the structure of atomic nuclei.

Atomic nuclei consist of protons and neutrons, collectively referred to as nucleons. The interaction between nucleons is dominated by the strong interaction, and nuclei as self-bound systems of nucleons form as the result of the strong interaction overcoming a strong kinetic repulsion due to nucleons being fermions and obeying the Pauli exclusion principle. Emergent out of the interplay between these two effects, with contributions from the weak and electromagnetic interactions, is the nuclear landscape, shown in Fig. 1.1. All of these isotopes arise out of the same basic physics, with constituent nucleons interacting via basic two- and three-particle interactions.

Ab initio nuclear theory aims to realize this understanding of the nuclear landscape in theoretical calculations, modeling nuclei from first principles using only the interactions between nucleons as input. Using only these interactions as inputs means that *ab initio* methods have far-reaching predictive power with a large range of applicability. An additional requirement for *ab initio* methods is that they are in a theoretical limit exact and

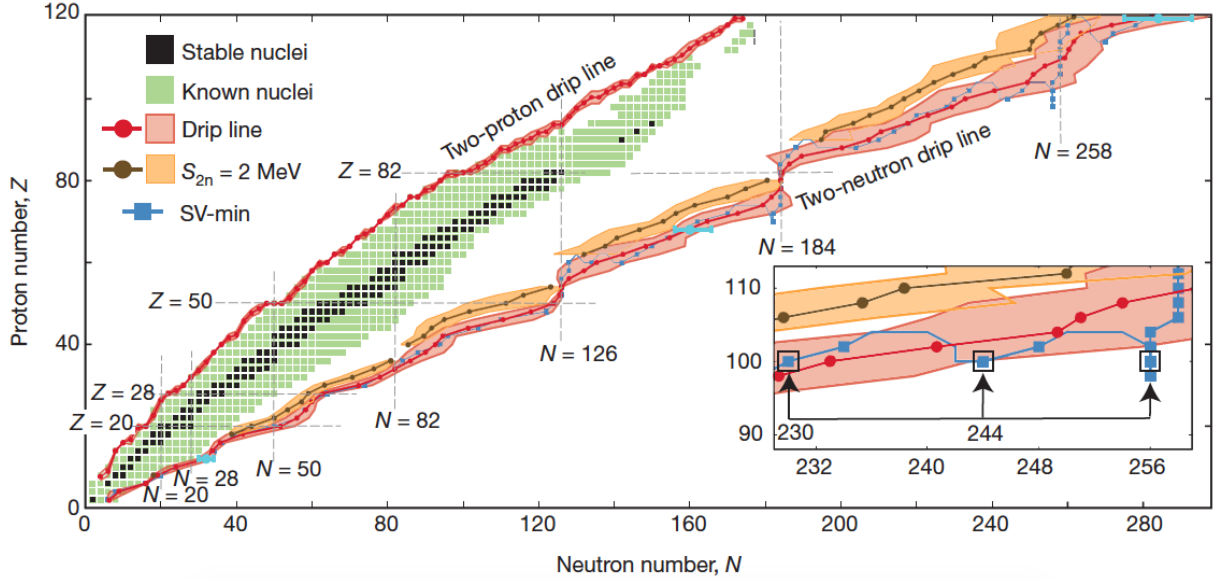


Figure 1.1: The nuclear landscape, with stable and unstable atomic nuclei denoted by the black and green squares, respectively, and a theoretical prediction of the limit of bound nuclei being indicated by the red bands. Figure taken from Ref. [2].

thus systematically improvable for any practical approximation. This feature also allows the *ab initio* approach to deliver robust uncertainty estimates, allowing for the meaningful comparison between experiment and theory and also between different *ab initio* theoretical approaches.

Over the past two decades, the range of *ab initio* results has expanded rapidly, as is shown in Fig. 1.2. This change was driven by shift in our understanding of *low-energy* nuclear physics, encapsulated in the effective field theory (EFT) and renormalization group (RG) methods. Underlying both of these ideas is the concept of limited resolution in low-energy physics and the realization that behavior at short distances (small wavelengths or high energies) does not affect the big picture at long distances. Effective field theory methods connect to underlying fundamental theories explicitly setting the scale to include essential long-distance physics and generating the most general expansion for the short-distance physics in terms of contact interactions [4, 5]. Renormalization group methods allow for varying of the resolution scale, decoupling or integrating out high-energy details to produce an efficient low-resolution description of the system at hand [6–8]. These two obviously synergistic methods have worked together to produce low-resolution nuclear forces rooted in the fundamental theory of quantum chromodynamics.

With these new, more efficient low-energy nuclear forces and the ever increasing available computational resources, the parallel development of nuclear many-body methods was uncapped. New developments on old methods, such as coupled cluster, and the in-

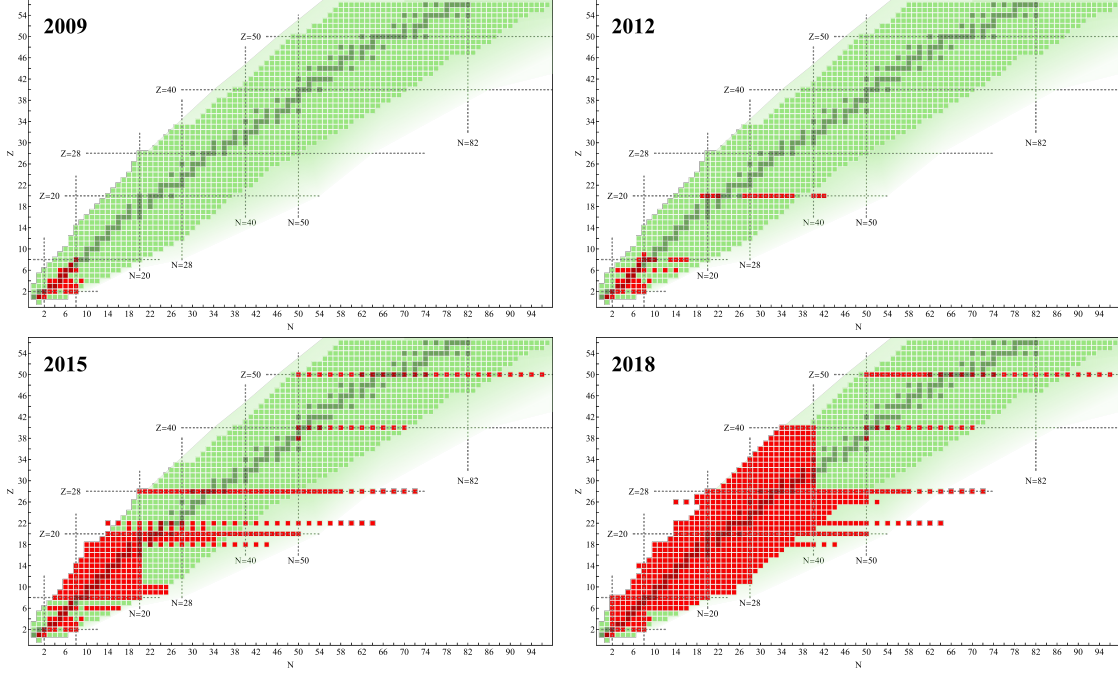


Figure 1.2: Chart of nuclides showing in red nuclei for which *ab initio* calculations involving two- and three-body interactions had been done in 2009 (top left) to 2018 (bottom right). Only calculations for which convergence with respect to basis size was achieved are included in the charts. Figure courtesy of Heiko Hergert [3].

roduction of new methods, such as the in-medium similarity renormalization group, have carried *ab initio* nuclear theory to its present state.

1.1 Goals

The focus of this work will be the in-medium similarity renormalization group (IM-SRG) [9]. As indicated by its name, it brings the RG approach of decoupling low- and high-energy states to the many-body problem, seeking to decouple the state of a system from its excitations. It is flexible in that it can target both ground states and low-lying excited states and calculate energies as well as expectation values for other operators, and while its original formulation centers on describing closed-shell nuclei, multiple variants are able to model open-shell nuclei as well.

The current state-of-the-art IM-SRG approaches truncate the formalism at the IM-SRG(2) level, the first non-trivial truncation where up to normal-ordered two-body operators are kept in the equations. This truncation has been quite successful, but for the purposes of reaching higher precision and allowing for quantification of many-body uncertainties, extending the truncation to the IM-SRG(3) level is of great interest. In this work, we aim to systematically study the improvements offered by the IM-SRG(3) for the

ground-state properties of light and medium-mass nuclei. As a step towards this goal, we also consider the simpler pairing Hamiltonian system in the IM-SRG.

1.2 Outline

The remainder of this thesis is structured as follows:

- In Chapter 2, we introduce some aspects of the theory of nuclear forces. We focus on the modern approaches to deriving nuclear forces and using choices to improve the convergence of many-body calculations.
- In Chapter 3, we introduce the many-body formalism that underlies the IM-SRG. We introduce some other many-body methods that also build on this formalism to help position the IM-SRG in the greater space of available many-body methods.
- In Chapter 4, we discuss the IM-SRG in detail. We discuss the general formalism and the IM-SRG(2) and IM-SRG(3) truncations. We also discuss generator choice, which sets how the IM-SRG decouples low and high energies, and the Magnus expansion, an extension that makes it easier to solve and easier to apply to other observables.
- In Chapter 5, we discuss the results of our application of our IM-SRG implementation. These results are primarily benchmarks to validate the correctness of our implementation.
- In Chapter 6, we summarize our results and offer an outlook for the next steps towards the goals of this thesis.

Chapter 2

Nuclear forces

For low-energy nuclear physics, the goal is to understand the structure and dynamics of systems with nucleons as constituents. Thus, a key input into any theoretical calculations of such systems is the interactions between nucleons. However, quantum chromodynamics (QCD), the theory of the strong interaction, is given in terms of quarks and gluons, not nucleons. Moreover, at low energies the strong interaction coupling constant $\alpha_s(q^2)$ becomes large, preventing a fundamental closed-form solution for the interactions between color-neutral hadrons.

As a result, various approaches to determine the interactions between nucleons have been developed. One such approach is the phenomenological expansion of the interaction between two nucleons into terms with different spin, isospin, and angular-momentum dependences. The (position- and momentum-dependent) strength of each of these terms is then fit to nucleon-nucleon scattering data, giving rise to, for example, the AV18 potential [10]. This approach has several features that make it undesirable for *ab initio* nuclear theory. First, it does not connect to the underlying fundamental theory. Second, this approach does not prescribe a way to arrive at consistent three-nucleon forces. Additionally, the fitting procedure often includes scattering data at relatively high energies when compared to the expected kinetic energy of nucleons in nuclei or nuclear matter, making such phenomenological interactions highly non-perturbative.

In this chapter, we discuss chiral effective field theory as an alternative to the phenomenological determination of nuclear forces and the similarity renormalization group as a method to generally “soften” interactions for many-body calculations. Then we discuss some details regarding different bases in which one can represent nuclear potentials.

2.1 Nuclear forces from chiral effective field theory

A modern approach to deriving nuclear potentials is chiral effective field theory. The EFT approach allows one to systematically construct a field theory that approximates a more fundamental theory in a low-energy domain [5, 12, 13]. In this appropriately chosen

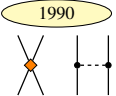
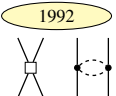
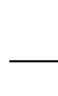
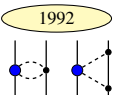
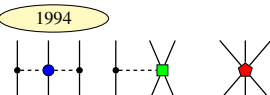
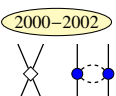

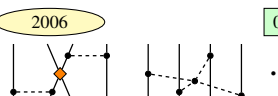
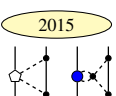
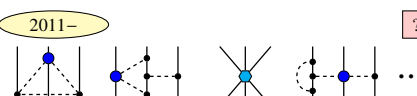

	NN	3N	4N
LO $\mathcal{O}(Q^0/\Lambda^0)$	 <div>1990</div> <div>2</div>	—	—
NLO $\mathcal{O}(Q^2/\Lambda^2)$	 <div>1992</div> <div>7</div>	 <div>1992, 1994</div>	—
N ² LO $\mathcal{O}(Q^3/\Lambda^3)$	 <div>1992</div> <div>0</div>	 <div>1994</div> <div>2</div>	—
N ³ LO $\mathcal{O}(Q^4/\Lambda^4)$	 <div>2000–2002</div> <div>12</div>	 <div>2008–2011</div> <div>0</div>	 <div>2006</div> <div>0</div>
N ⁴ LO $\mathcal{O}(Q^5/\Lambda^5)$	 <div>2015</div> <div>0</div>	 <div>2011–</div> <div>?</div>	 <div>?</div>

Figure 2.1: The contributions to NN, 3N, and 4N interactions in chiral EFT up to order N4LO. Solid lines indicate nucleon propagators. Dashed lines indicate pion propagators. The number of new LECs for the new interaction contributions at each new order is shown in the top right corner. Figure taken from Ref. [11].

domain, one can use the most efficient degrees of freedom to formulate the theory. The construction of the theory relies on knowing the symmetries (exact and approximate) of the underlying theory. Constructing the most general Lagrangian consistent with these underlying symmetries yields the most general S -matrix [4].

To construct an effective field theory, one identifies the degrees of freedom one wants to work with and identifies a high-momentum scale Λ of the underlying theory that characterizes physics no longer resolved by the EFT [5]. The EFT then should be an efficient, approximately complete description of the relevant physics at momenta Q small compared to Λ . The chosen degrees of freedom are used to construct the most general Lagrangian consistent with the underlying symmetries, which will have an infinite number of terms each with their own coefficients, the so-called low-energy constants (LECs). The EFT can then be used to calculate observables up to some precision in an expansion in Q/Λ , made systematic by a power-counting approach.

For chiral EFT, the underlying theory is QCD in the light-quark sector (here this means only up and down quarks), where the Lagrangian has an approximate chiral symmetry $SU(2)_L \times SU(2)_R$ in the limit of vanishing quark masses and no electroweak interactions [5]. This symmetry is spontaneously broken, giving rise to the pion as the Goldstone boson associated with the broken $SU(2)_A$ symmetry, as well as explicitly broken by the non-zero

quark masses [14]. A logical choice of degrees of freedom is then nucleons and pions. The high-momentum scale Λ_b is set by the lightest meson not included in our degrees of freedom, the ρ meson with a mass of $m_\rho \approx 770$ MeV [13]. The low-momentum scale is a collective scale given by $\max(Q, m_\pi)$.

The resulting potential contributions from chiral EFT have either explicit pion exchanges or contact interactions with LECs describing short-range physics unresolved by the EFT, as shown in Fig. 2.1. The first consistent three-nucleon (3N) interactions appear at next-to-next-to-leading order (N2LO), and the first four-nucleon (4N) interactions appear at next-to-next-to-next-to-leading order (N3LO). Among the features that make EFTs so powerful is that they allow for clear error estimates [15–17], given proper power-counting, by considering the order-by-order convergence of observables and seeing that the orders left out due to a truncation at order N should contribute something like

$$\Delta O^{(N)} \sim O\left(\frac{\max(Q, m_\pi)}{\Lambda_b}\right)^{N+1}, \quad (2.1)$$

where O is the exact result for some observable of interest (see Fig. 2.2).

For potentials from chiral EFT, at each order a finite number of undetermined LECs are introduced with the new contributions to the potential. For nucleon-nucleon (NN) interactions, these can be determined by fitting to *low-energy* scattering data. For 3N interactions, the relevant LECs must be fit to three-body or four-body observables. Typical choices for these observables at N2LO, where two three-body LECs, c_D and c_E , need to be fit, are the triton binding energy and either the triton half-life or the ^4He charge radius [11]. Additionally, some contributions at later orders in the expansion only depend on LECs from previous orders. For example, the 3N force contributions at N3LO require no new LECs to be fit.

Some comments are now in order regarding interactions as used in this thesis. The derivation of potentials requires the explicit regularization of momenta to make divergent integrals over intermediate momenta convergent. This introduces a dependence on the regularization scheme and scale used, which is an artifact of the finite order of our EFT. Each additional order in the EFT cancels the scale dependence of the previous order, and in the limit of infinite order all observables should not depend on the cutoff scale and scheme used (within reason). For every interaction used we state the order, the regularization scale, and the family of interactions, which specifies the regularization scheme used.

We use primarily two families of interactions. The first set is a family of interactions with NN interactions given up to N3LO which was worked out by Entem and Machleidt in 2003 [18]. These interactions are denoted by EM when they are used. The second set was worked out by Entem, Machleidt, and Nosyk in 2017 and provides NN interactions up to N4LO [19]. These interactions are denoted by EMN. From 2007 through 2011, the 3N interactions were worked out [20–22], and the consistent (in terms of power-counting and regularization scheme) 3N potentials with these families up to N3LO were presented in 2015 by Hebeler *et al.* [23]. At N3LO, the chiral power-counting dictates the inclusion

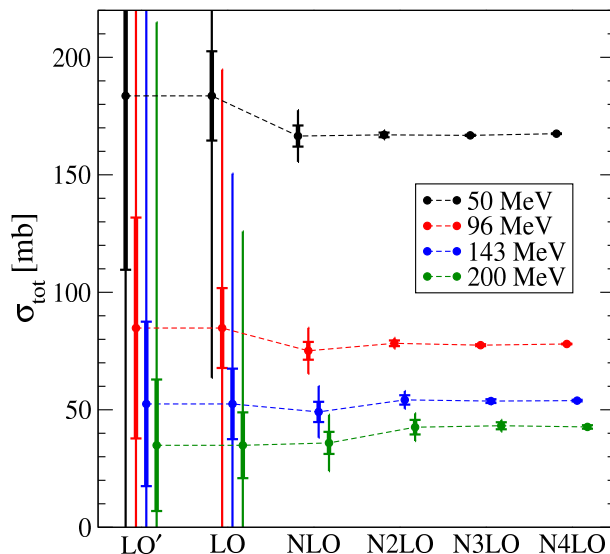


Figure 2.2: The total proton-neutron scattering cross section calculated order by order at different energies using potentials from Ref. [17] with 68% and 95% degree of belief intervals indicated by the thick and thin error bars obtained via Bayesian uncertainty quantification [15]. Figure taken from Ref. [15].

of 4N forces (see Fig. 2.1). However, this is generally *not* done because the inclusion of 4N forces in calculations is prohibitively expensive and past results have shown that they contribute at the sub-1% level [24, 25].

Chiral EFT essentially resolves all of the shortcomings of phenomenological potentials mentioned previously. There are still many open questions regarding the derivation of potentials via chiral EFT and their consistent application in many-body calculations. For example, there are multiple schools of thought regarding what the correct power-counting for nuclear potentials is [26–28]. Additionally, the uncertainties from the regularization scheme and scale for nuclear potentials are still most likely dominant in many-body calculations. However, the rapid expansion of the range of *ab initio* calculations over the past two decades has been in no small part due to the introduction of chiral potentials and the development of auxiliary tools to aid in their application to many-body calculations.

2.2 Similarity renormalization group evolution of nuclear forces

The similarity renormalization group (SRG) is a method that has been used to great success to “soften” nuclear interactions [7, 29, 30]. The key idea of the SRG is the generation of a continuous unitary transformation of a given Hamiltonian,

$$H(s) = U(s) H U^\dagger(s), \quad (2.2)$$

where s is the continuous flow parameter. The resulting flow equation gives the evolution of the Hamiltonian

$$\frac{dH(s)}{ds} = [\eta(s), H(s)], \quad (2.3)$$

with $\eta(s) = U(s)dU^\dagger(s)/ds$ and we choose $H(0) = H$. An “appropriate” choice of the anti-Hermitian generator η can generate a unitary transformation such that $H(s)$ evolves, for example, towards a diagonal form. This leads to a decoupling of low- and high-energy states in the Hamiltonian, allowing for a truncation in momentum space or a discretized basis without distorting low-energy observables.

The evaluation of the commutator in the SRG flow equation generates higher-body forces in the evolved Hamiltonian, even if the initial Hamiltonian consists only of two- and three-body forces. This means that the fully unitary SRG evolution of an A -body Hamiltonian requires the evaluation of the flow equation in the A -body basis. For all but the smallest systems, this is computationally infeasible.

A pragmatic approach uses the SRG restricted to the three-body space to evolve two- and three-body nuclear forces to “softer” forms in momentum space [31], reducing coupling between low- and high-energy states. These evolved potentials are for few-body purposes equivalent to the un-evolved (“bare”) ones, reproducing the few-body binding energies, radii, and NN phase shifts exactly. After truncating the potentials, taking advantage of the decoupling, the few-body observables remain essentially unchanged, and the low-energy NN phase shifts are also preserved.

The typical choice for the generator in the so-called “free space” SRG in nuclear applications is

$$\eta(s) = [T_{\text{rel}}, H(s)], \quad (2.4)$$

where T_{rel} is the relative kinetic energy of the two- and three-body systems. In two-body Jacobi momentum coordinates, T_{rel} is diagonal, thus the right-hand side of the flow equation clearly has a fixed point if $H(s)$ is ever diagonal. Evaluating the flow equation in momentum space in the two-body case for this choice for η gives

$$\frac{dV_2(s; p, p')}{ds} = -(p^2 - p'^2)^2 V_2(s; p, p') + \int dp'' (p^2 + p'^2 - 2p''^2) V_2(s; p, p'') V_2(s; p'', p'), \quad (2.5)$$

where p and p' are the incoming and outgoing Jacobi momenta of the two-body subsystem (see Section 2.3.1). We also used the conventional choice of leaving the kinetic energy invariant under the SRG evolution. Empirically, one can see that the first term dominates the evolution for far off-diagonal elements in nuclear applications, and so

$$V_2(s; p, p') \approx V_2(0; p, p') \exp(-s(p^2 - p'^2)^2). \quad (2.6)$$

Using a redefinition of the flow parameter

$$\lambda = \frac{1}{s^{1/4}}, \quad (2.7)$$

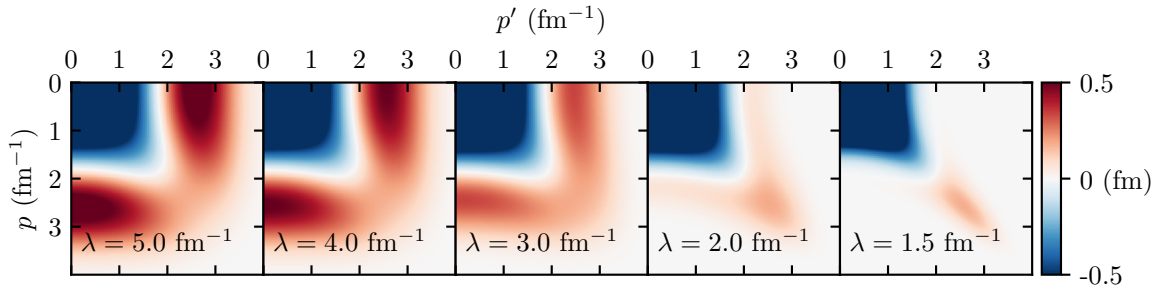


Figure 2.3: An example of an SRG-evolved potential using the chiral NN potential from Ref. [19] at N4LO in the 3S_1 part of the 3S_1 - 3D_1 channel.

which has units of fm^{-1} and evolves from $\lambda = \infty$ towards 0, one can see that over the course of the evolution off-diagonal parts of the potential outside a band of width λ begin to be exponentially suppressed [32]. Looking at Fig. 2.3, one can see that this is qualitatively true, and the desired decoupling between low- and high-momentum states is achieved.

These softened interactions can then be fed into many-body frameworks, which benefit strongly from the improved convergence with respect to modelspace size. However, the few-body evolution of potentials neglects induced A -body forces, which do contribute in many-body calculations. One way to probe the size of the missing many-body forces is to do calculations with potentials evolved to different values of s or λ and see how much the calculated result depends on the renormalization scale. A strong dependence would indicate significant missing contributions from many-body forces while no dependence would indicate approximate renormalization group invariance, which is ultimately the goal [8].

2.3 Representations of nuclear potentials

The efficient representation of nuclear potentials exploits symmetries of the few-body system and the interactions. In particular, for 3N forces, where the potential can depend in principle on 18 parameters in momentum space $(\vec{k}_1, \vec{k}_2, \vec{k}_3, \vec{k}'_1, \vec{k}'_2, \vec{k}'_3)$, simplifications afforded by these symmetries are essential to being able to evaluate, store, and calculate with these potentials.

The essential symmetries of the free two- and three-nucleon systems (from which the potentials are determined) are

- conservation of the center-of-mass momentum of the system,
- independence on the center-of-mass momentum,
- and rotational invariance [11].

Additionally, one can simplify things dramatically by making the assumption that the masses of all nucleons are the same, a reasonable assumption given that the mass difference between the proton and neutron is less than a per mille [11]. In this approximation in the absence of electroweak interactions, the NN force would also be independent of isospin projection, however the Coulomb interaction breaks this isospin charge symmetry. Also, even without the Coulomb interaction, the chiral EFT expansion explicitly breaks isospin charge symmetry at higher orders, a result of it being constructed in a way that systematically accounts for the breaking of approximate symmetries. However, at the orders in chiral EFT considered here, such isospin charge symmetry violating processes do not contribute.

In the following, we discuss some possible representations of NN forces, going from one of the representations most convenient for the evaluation of potentials to the representation of choice for the many-body methods discussed in this thesis. We mention along the way some of the analogous results for 3N forces. A more thorough treatment of this topic can be found in Ref. [11].

2.3.1 Jacobi momentum space

Going from single-particle momenta to Jacobi and center-of-mass momenta, like

$$\vec{k}_1, \vec{k}_2 \rightarrow \vec{p}, \vec{P}_{2N}, \quad (2.8)$$

$$\vec{k}_1, \vec{k}_2, \vec{k}_3 \rightarrow \vec{p}, \vec{q}, \vec{P}_{3N}, \quad (2.9)$$

allows one to factor out and ignore the center-of-mass degrees of freedom of the system. The Jacobi and center-of-mass momenta are defined as

$$\vec{p} = \frac{\vec{k}_1 - \vec{k}_2}{2}, \quad (2.10)$$

$$\vec{P}_{2N} = \vec{k}_1 + \vec{k}_2, \quad (2.11)$$

$$\vec{q} = \frac{2\vec{k}_3 - \vec{P}_{2N}}{3}, \quad (2.12)$$

$$\vec{P}_{3N} = \vec{k}_1 + \vec{k}_2 + \vec{k}_3. \quad (2.13)$$

For NN forces, this gives us two-body states of the form

$$|\vec{p} s_1 m_{s_1} s_2 m_{s_2} t_1 m_{t_1} t_2 m_{t_2}\rangle, \quad (2.14)$$

where $s_i = 1/2$, m_{s_i} , $t_i = 1/2$, m_{t_i} are the i -th particle's spin, spin projection, isospin, and isospin projection, respectively. In cases where explicit values of isospin projection are used, we adopt the convention that for protons $m_t = 1/2$ and for neutrons $m_t = -1/2$.

To take advantage of rotational invariance, one can decompose the potential into partial-wave channels, with two-body states like

$$|p [l (s_1 s_2) S] J m_J T m_T\rangle, \quad (2.15)$$

where p is the magnitude of \vec{p} , l is the relative orbital angular momentum of the two-body system, and S , J , m_J , T , m_T are the total spin, total angular momenta, total angular momentum projection, isospin, and isospin projection of the two-body system. The resulting potential

$$\langle p' [l' (s'_1 s'_2) S'] J' m'_J T' m'_T | V_{2N} | p [l (s_1 s_2) S] J m_J T m_T \rangle \quad (2.16)$$

is proportional to $\delta_{JJ'} \delta_{m_J m_{J'}}$ and independent of m_J due to rotational invariance. Additionally, antisymmetry under exchange of particle indices and parity conservation require it to also be proportional to $\delta_{SS'} \delta_{TT'}$ with the additional constraints

$$(-1)^{l+S+T+1} = (-1)^{l'+S+T+1} = 1, \quad (2.17)$$

$$l - l' = -2, 0, 2, \quad (2.18)$$

and charge conservation requires that it also is proportional to $\delta_{m_T m_{T'}}$. For notational convenience, we sometimes collect the partial-wave quantum numbers of states in a collective index α_2 , allowing the concise notation for 2N potentials

$$\langle p' \alpha'_2 | V_{2N} | p \alpha_2 \rangle. \quad (2.19)$$

With this, the representation of NN forces has been reduced to two continuous variables, p and p' , and some strongly constrained partial-wave quantum numbers. For 3N forces, there is similar simplification possible, yielding three-body states of the form

$$|pq [(lS) J (\ell s) j] \mathcal{J} \mathcal{M}_{\mathcal{J}} (Tt) \mathcal{T} \mathcal{M}_{\mathcal{T}} \rangle, \quad (2.20)$$

where p, l, S, J, T still refer to the two-particle subsystem as before, q, ℓ, j are the Jacobi momentum, orbital angular momentum, and total angular momentum of the third nucleon relative to the two-body subsystem center-of-mass, and s and t are the spin and isospin of the third nucleon. Here, the 3N potential is, among other things, independent of $\mathcal{M}_{\mathcal{T}}$.

2.3.2 Jacobi harmonic-oscillator space

The transformation to Jacobi harmonic-oscillator (HO) space follows quite simply. Using the radial solutions to the isotropic three-dimensional harmonic oscillator with frequency $\hbar\Omega$, one obtains

$$\langle n' \alpha'_2 | V_{2N} | n \alpha_2 \rangle = \int dp p^2 dp' p'^2 R_{n'v'}(p') R_{nl}(p) \langle p' \alpha'_2 | V_{2N} | p \alpha_2 \rangle. \quad (2.21)$$

The radial solutions are given by

$$R_{nl}(p) = \sqrt{\frac{2(n!)}{(m\hbar\Omega)^{3/2} \Gamma(n+l+3/2)}} (\tilde{p})^l \exp(-\tilde{p}^2/2) L_n^{l+1/2}(\tilde{p}^2), \quad (2.22)$$

where m is the nucleon mass, $\tilde{p} = p/\sqrt{m\hbar\Omega}$ is the dimensionless momentum, and $L_n^k(x)$ are the generalized Laguerre polynomials. For 3N forces, the Jacobi momenta q and q' must also be transformed, giving two more integrals.

In the infinite modelspace limit, this transformation is exact, and the dependence on the basis frequency $\hbar\Omega$ disappears. However, for practical calculations a basis truncation n_{\max} must be introduced, which implicitly introduces an ultraviolet (UV) cutoff and an infrared (IR) cutoff. The UV cutoff is due to high frequencies requiring HO wave functions beyond the truncation to be resolved. The IR cutoff is due to the basis frequency $\hbar\Omega$ setting the minimum frequency reproducible by wave functions in the basis.

For a given truncation, the optimal $\hbar\Omega$ can be determined by making use of the variational principle, which states that for the true ground state the energy functional $E[|\psi\rangle]$ is stationary under infinitesimal variations of $|\psi\rangle$. In this case, one can look at the approximate ground state by solving the two- or three-body system (for example, via exact diagonalization). For the optimal $\hbar\Omega$, the ground-state energy will be minimal, guaranteed by the variational principle to be no less than the true ground-state energy. Many-body calculations are typically done with operators transformed at several $\hbar\Omega$. For energies the minimum result under this variation is taken to be the result of the calculation, but it is important to note that many many-body methods are *not* variational.

2.3.3 Single-particle harmonic-oscillator space

Many many-body methods used in nuclear physics, in particular also wave function expansion methods, work with operators given in a single-particle basis as input. This means we have a basis of single-particle states

$$\{|a\rangle\} \tag{2.23}$$

spanning the one-body Hilbert space. Then the set of product states

$$|ab\rangle = |a\rangle |b\rangle \tag{2.24}$$

spans the two-body Hilbert space. At this point these states are not appropriately antisymmetrized. At the end of this section, we discuss how to recover the required antisymmetry under exchange of particle indices.

In our case, we work with the single-particle harmonic-oscillator basis with the same frequency $\hbar\Omega$ as used in the transformation above. To be explicit, these states are of the form

$$|n_a(l_a s_a) j_a m_{j_a} t_a m_{t_a}\rangle . \tag{2.25}$$

The two-body single-particle states are then

$$|n_a(l_a s_a) j_a m_{j_a} t_a m_{t_a} n_b(l_b s_b) j_b m_{j_b} t_b m_{t_b}\rangle , \tag{2.26}$$

or, coupled to two-body total angular momentum J ,

$$|n_a n_b [(l_a s_a) j_a (l_b s_b) j_b] J m_J t_a m_{t_a} t_b m_{t_b}\rangle . \quad (2.27)$$

To connect the states in Eq. 2.26 with those in Eq. 2.21, one does a Talmi-Moshinsky transformation. This connects the relative and center-of-mass excitation numbers, n and N , and orbital angular momentum numbers, l and L , with the single-particle excitation numbers, n_a and n_b , and orbital angular momentum numbers, l_a and l_b . The central object of this transformation is the harmonic-oscillator bracket

$$\langle n_a n_b (l_a l_b) \Lambda | n N (l L) \Lambda \rangle , \quad (2.28)$$

where both sets of orbital angular momenta have been coupled to total orbital angular momentum Λ . The properties and evaluation of these brackets is discussed in detail in Refs. [33, 34]. By appropriately decoupling and recoupling angular momenta and applying the harmonic-oscillator brackets, one arrives at NN potential matrix elements of the form

$$\langle ab | V_{2N} | cd \rangle , \quad (2.29)$$

where a , b , c , and d are collective indices that run over the single-particle states in Eq. 2.25.

The matrix elements in Eq. 2.29 do not obey the required antisymmetry of fermions under exchange of particle indices since the product states $|ab\rangle$ are not antisymmetrized. Restoring the required antisymmetry, one obtains the antisymmetrized matrix elements

$$V_{2N,abcd} = \frac{1}{2}(1 - P_{ab})(1 - P_{cd}) \langle ab | V_{2N} | cd \rangle \quad (2.30)$$

$$= (1 - P_{cd}) \langle ab | V_{2N} | cd \rangle , \quad (2.31)$$

where P_{ab} exchanges the indices a and b in the following expression. The simplification above takes advantage of the symmetry

$$\langle ab | V_{2N} | cd \rangle = \langle ba | V_{2N} | dc \rangle , \quad (2.32)$$

arising due to the indistinguishability of the two particles. In the next chapter, we develop the fundamentals of the formalisms that use these matrix elements as input.

Chapter 3

Many-body basics and wave function expansion methods

The goal of many-body quantum mechanics is to solve the A -body time-independent Schrödinger equation. This requires, among other things, the construction of a set of states that span the A -body Hilbert space. For distinguishable particles, taking a set of single-particle states $|p\rangle$ and building A -body product states $|p_1\rangle \dots |p_A\rangle$ would be a reasonable approach. However, the wave function of a system of A nucleons, which are indistinguishable fermions, must be antisymmetric under the exchange of any two particle labels. The explicit antisymmetrization of states going from naive product states quickly becomes unwieldy with growing A .

Second quantization offers an alternative that bakes the required antisymmetry into the formalism. This formalism is the basis for a class of many-body methods called wave function expansion methods, which includes the IM-SRG. These methods have the benefit that, instead of scaling combinatorially in A like exact diagonalization approaches, they scale polynomially, taking advantage of knowledge of a good approximate solution to the ground state to reduce the task to finding corrections to this zeroth-order ansatz. In this chapter, we introduce the basics of second quantization and normal ordering, focusing on the case of fermions. Then we discuss some of the more traditional wave function expansion methods before discussing the IM-SRG in detail in the next chapter.

3.1 Second quantization

To consider second quantization, one starts by constructing the Fock space, the direct sum of all A -body antisymmetric Hilbert spaces. As a concrete example, for the zero-, one-, and two-body Hilbert spaces, we have the bases

$$A = 0 \rightarrow |0\rangle, \tag{3.1}$$

$$A = 1 \rightarrow \{|p\rangle\}, \tag{3.2}$$

$$A = 2 \rightarrow \left\{ \frac{|p\rangle_1 |q\rangle_2 - |q\rangle_1 |p\rangle_2}{\sqrt{2}} \mid q > p \right\} . \quad (3.3)$$

These states (and many more) are all in the Fock space, related to one another via field operators.

The field operators are particle creation and annihilation operators that connect states in the A -body antisymmetric Hilbert space to states in the $A + 1$ -body and $A - 1$ -body antisymmetric Hilbert spaces. The creation operator a_p^\dagger creates a particle in the single-particle state $|p\rangle$. Operating on an A -body state with it creates an $A + 1$ -body state with an additional particle in state $|p\rangle$,

$$a_p^\dagger |p_1 \dots p_A\rangle_a = (1 - n_p) |pp_1 \dots p_A\rangle_a , \quad (3.4)$$

where we have explicitly denoted that the states are antisymmetrized. Here, n_p is the occupation number of state $|p\rangle$ in the A -body state, which for fermions, due to the Pauli exclusion principle, can only be 0 or 1. Attempting to create a second particle in an already occupied state annihilates the state.

The annihilation operator a_p annihilates a particle in the single-particle state $|p\rangle$. Operating on an A -body state with it creates an $A - 1$ -body state with a particle in state $|p\rangle$ removed,

$$a_p |pp_2 \dots p_A\rangle_a = n_p |p_2 \dots p_A\rangle_a . \quad (3.5)$$

If no particle with the single-particle state $|p\rangle$ exists in the state, the annihilation operator annihilates the state.

With the field operators, an antisymmetric A -body state can very efficiently be written as

$$|p_1 p_2 \dots p_A\rangle_a = a_{p_1}^\dagger a_{p_2}^\dagger \dots a_{p_A}^\dagger |0\rangle . \quad (3.6)$$

This antisymmetrized product of A particles in A unique single-particle states is frequently referred to as a Slater determinant, owing to the fact that it can be, in its explicitly antisymmetrized form, written as an appropriately normalized determinant [35].

Since these states should be antisymmetric under exchange of particle indices, that is,

$$|p_1 p_2 \dots p_A\rangle_a = - |p_2 p_1 \dots p_A\rangle_a , \quad (3.7)$$

the creation and annihilation operators must anti-commute with themselves,

$$\{a_p^\dagger, a_q^\dagger\} = 0 , \quad (3.8)$$

$$\{a_p, a_q\} = 0 . \quad (3.9)$$

Similarly, one can arrive at the anti-commutation relation between creation and annihilation operators,

$$\{a_p, a_q^\dagger\} = \delta_{pq} . \quad (3.10)$$

With this formalism in place, we are now in a position to discuss the representation of many-body operators in the Fock space. Operators are classified as A -body operators if they can at most couple A particles. We have used this language frequently so far, but we make it very precise in the following discussion.

Zero-body operators are simple scalars,

$$O^{(0)} = o. \quad (3.11)$$

They have, among other things, in general a non-zero vacuum expectation value.

One-body operators are of the form

$$O^{(1)} = \sum_{pq} O_{pq}^{(1)} a_p^\dagger a_q, \quad (3.12)$$

where $O_{pq}^{(1)}$ are the matrix elements of $O^{(1)}$. One-body operators have two useful properties. First, their vacuum expectation value is 0:

$$\langle 0 | O^{(1)} | 0 \rangle = 0. \quad (3.13)$$

Second, they do not contribute to processes where the incoming (bra) and outgoing (ket) states differ in more than one single-particle state. Some examples of one-body operators are the kinetic energy and an external potential.

Two-body operators are of the form

$$O^{(2)} = \frac{1}{(2!)^2} \sum_{pqrs} O_{pqrs}^{(2)} a_p^\dagger a_q^\dagger a_s a_r. \quad (3.14)$$

Here $O_{pqrs}^{(2)}$ is an antisymmetrized matrix element, with the property

$$O_{pqrs}^{(2)} = -O_{qprs}^{(2)} = -O_{psrq}^{(2)} = O_{rpsq}^{(2)}. \quad (3.15)$$

We note that in Eq. 3.14 the order of the annihilation operators is reversed relative to the indices on the matrix element. The indices p and r and the indices q and s are “paired,” and the product of creation and annihilation operators is structured such that the pairs are nested inside of each other, not adjacent to each other. However, by the antisymmetry of the matrix elements, the matrix element for one pairing determines it for all other pairings of the same creation and annihilation operators. Two-body operators have the properties

$$\langle 0 | O^{(2)} | 0 \rangle = 0, \quad (3.16)$$

$$\langle p | O^{(2)} | q \rangle = 0, \quad (3.17)$$

and they do not contribute to processes where incoming and outgoing states differ in more than two single-particle states. A typical example of a two-body operator is any pairwise interaction, such as the Coulomb interaction or NN nuclear forces.

Three-body operators are of the form

$$O^{(3)} = \frac{1}{(3!)^2} \sum_{pqrstu} O_{pqrstu}^{(3)} a_p^\dagger a_q^\dagger a_r^\dagger a_u a_t a_s. \quad (3.18)$$

Here, $O_{pqrstu}^{(3)}$ are also antisymmetrized matrix elements, with the property

$$O_{pqrstu}^{(3)} = (-1)^{\sigma_1} (-1)^{\sigma_2} O_{\sigma_1(pqr)\sigma_2(stu)}^{(3)}, \quad (3.19)$$

where σ_1 and σ_2 are permutations and the $(-1)^\sigma$ prefactors account for the signs of the permutations. Three-body operators have the properties

$$\langle 0 | O^{(3)} | 0 \rangle = 0, \quad (3.20)$$

$$\langle p | O^{(3)} | q \rangle = 0, \quad (3.21)$$

$$\langle pq | O^{(3)} | rs \rangle = 0, \quad (3.22)$$

and they do not contribute to processes where incoming and outgoing states differ in more than three single-particle states. Examples of three-body operators are 3N nuclear forces. These definitions can be generalized to get the general representation of any A -body operator, and the properties follow analogously.

3.2 Normal ordering

A product of creation and annihilation operators is in normal order if all creation operators appear to the left of all annihilation operators. The normal ordering operation on cA , where c is a scalar coefficient and A is a product of creation and annihilation operators, can be written as

$$N[cA] = (-1)^\sigma c\sigma(A) \quad (3.23)$$

where σ is a permutation that rearranges the product A into normal order. This rearrangement is not unique, but, since each change in the permutation is accompanied by a change in the exchange prefactor, all normal-ordered products resulting from different permutations used in normal ordering are equivalent. Also, note that in general $N[A] \neq A$, since anti-commuting creation and annihilation operators past each other will leave a residual δ_{pq} from their anti-commutation relation.

3.2.1 General properties

Suppose the product of creation and annihilation operators A contains p creation operators and q annihilation operators. Then, unless p and q are both 0, $N[A]$ has a vacuum expectation value of 0. Additionally, $N[A]$ does not contribute to processes where the incoming state has less than q particles or the outgoing state has less than p particles.

We are now interested in considering products of normal-ordered products of creation and annihilation operators. Ultimately, we will use Wick's theorem to systematically

evaluate these products [36]. To introduce the theorem, we first need to introduce the notion of a Wick contraction, which for adjacent operators α and β is defined as

$$\overline{\alpha\beta} = \alpha\beta - N[\alpha\beta] . \quad (3.24)$$

The value of the contraction is the vacuum expectation value of $\alpha\beta$. Note that for two operators that are already in normal order their contraction vanishes. This provides an alternative definition of normal ordering, namely a product of two operators is in normal order if its vacuum expectation value is 0 and so its contraction vanishes. This leads to an extension of normal ordering that works for many different vacuum choices, including multi-reference vacuums which we don't consider any further in this work [37].

We are now equipped to use Wick's theorem to rewrite a general product of creation and annihilation operators in terms of sums of normal-ordered products and contractions:

$$\begin{aligned} ABCDEF \dots = & N[ABCDEF \dots] \\ & + \overline{AB} N[CDEF \dots] - \overline{AC} N[BDEF \dots] + \text{singles} \\ & + \left(\overline{ABCD} - \overline{ACBD} + \overline{ADBC} \right) N[EF \dots] + \text{doubles} \\ & + \dots + \text{full contractions} . \end{aligned} \quad (3.25)$$

The minus signs arise due to the fact that in order to simplify the contraction and pull it out of the normal-ordered product, we must anti-commute the contracted operators such that they are adjacent.

The generalized Wick's theorem states that for a product of two normal-ordered products of creation and annihilation operators, $A = N[A_1 A_2 \dots A_N]$ and $B = N[B_1 B_2 \dots B_M]$, the resulting expression in terms of normal-ordered products is the sum of all normal-ordered terms with 0 to $\min(N, M)$ contractions between the operators in A and B , that is,

$$\begin{aligned} N[A_1 A_2 \dots A_N] N[B_1 B_2 \dots B_M] = & N[A_1 A_2 \dots A_N B_1 B_2 \dots B_M] \\ & + (-1)^{N-1} \overline{A_1 B_1} N[A_2 \dots A_N B_2 \dots B_M] \\ & + (-1)^{N-2} \overline{A_2 B_1} N[A_1 \dots A_N B_2 \dots B_M] \\ & + (-1)^N \overline{A_1 B_2} N[A_2 \dots A_N B_1 \dots B_M] \\ & + (-1)^{N-1} \overline{A_2 B_2} N[A_1 \dots A_N B_1 \dots B_M] \\ & + \text{singles} + \text{doubles} + \dots . \end{aligned} \quad (3.26)$$

Despite the name, this is a special case of Eq. 3.25.

3.2.2 Vacuum normal ordering

In Section 3.2.1, we discussed the properties of normal ordering in general, and while we referenced “the vacuum” several times (for example, in the context of vacuum expectation

values), we never specified the specific vacuum involved. Indeed, normal ordering is dependent on the vacuum with respect to which it is done, and there are multiple options for this vacuum. In the following, we focus on normal ordering with respect to the *physical* vacuum $|0\rangle$, that is, the state with no particles present.

The fermion creation and annihilation operators a_p^\dagger and a_p are the *physical* creation and annihilation operators, so normal ordering with respect to the physical vacuum, which we denote by $N_0[\dots]$, produces products with all creation operators to the left of annihilation operators. Concretely, one can consider adjacent Wick contractions, which should be 0 for pairs of operators already in normal order. Applying the definition that a contraction of two adjacent operators is the vacuum expectation value of the operator product, we find

$$\underline{a_p a_q^\dagger} = \langle 0 | a_p a_q^\dagger | 0 \rangle = \delta_{pq}, \quad (3.27)$$

where we use the contraction *below* to indicate that we are normal ordering with respect to the physical vacuum. Similarly, we find

$$\underline{a_p a_q} = 0, \quad (3.28)$$

$$\underline{a_p^\dagger a_q^\dagger} = 0, \quad (3.29)$$

$$\underline{a_p^\dagger a_q} = 0, \quad (3.30)$$

indicating that these products are already in normal order, as expected.

As a brief aside, the definitions for the second-quantized form of one-, two-, and three-body operators in Eqs. 3.12, 3.14, and 3.18 are clearly already in normal order with respect to the physical vacuum. This is no longer the case when we normal order with respect to some other vacuum.

3.2.3 In-medium normal ordering

One alternative is normal ordering with respect to an A -body reference state, also called the Fermi vacuum, given by

$$|\Phi\rangle = \prod_{i=1}^A a_{p_i}^\dagger |0\rangle. \quad (3.31)$$

The frequently used occupation numbers for single-particle states in the reference state n_p are then

$$n_p = \begin{cases} 1 & p \in \{p_i\}, \\ 0 & p \notin \{p_i\}. \end{cases} \quad (3.32)$$

When calculating operator matrix elements for an A -body system, every bra or ket state comes with A annihilation or creation operators along with the physical vacuum. A more practical, but equivalent way to go about this is constructing A -body states from the reference state $|\Phi\rangle$, annihilating states occupied in the reference state but unoccupied in

the state of interest and creating in their place particles occupied in the state of interest. As an example, an A -body state that differs from the reference state by one single-particle state is given by

$$a_a^\dagger a_i |\Phi\rangle \equiv |\Phi_i^a\rangle. \quad (3.33)$$

One thing to note is that with respect to the reference state, the fermion creation and annihilation operators no longer have certain useful properties. For example, the annihilation operator no longer always annihilates the Fermi vacuum, and the creation operator in some cases *does* annihilate the Fermi vacuum. However, one can define quasiparticle creation and annihilation operators that recover these properties with respect to the reference state, with the annihilation operator given by

$$b_p = \begin{cases} a_p & \text{if } p \text{ is unoccupied in the reference state,} \\ a_p^\dagger & \text{if } p \text{ is occupied in the reference state,} \end{cases} \quad (3.34)$$

and the creation operator being related by conjugation.

These quasiparticle field operators obey all the typical anti-commutation relations and have the usual properties, just with respect to the reference state:

$$\{b_p, b_q^\dagger\} = \delta_{pq}, \quad (3.35)$$

$$\{b_p, b_q\} = 0, \quad (3.36)$$

$$\{b_q^\dagger, b_q^\dagger\} = 0, \quad (3.37)$$

$$b_p |\Phi\rangle = 0, \quad (3.38)$$

$$b_p^\dagger |\Phi\rangle \neq 0. \quad (3.39)$$

The quasiparticle creation operator b_p^\dagger annihilates a particle in the reference state if the state p is occupied, producing a so-called hole state. But when p is unoccupied in the reference state, b_p^\dagger creates a particle. This gives this formalism its name, the particle-hole formalism.

In this thesis so far, we have used indices p, q, r, \dots to indicate that the indices run over all single-particle states. Here we introduce the convention that the indices i, j, k, \dots only run over hole states, that is, states that are occupied in the reference state, and the indices a, b, c, \dots only run over particle states, that is, states that are unoccupied in the reference state.

We are now interested in normal ordering with respect to our reference state, which we denote by $N_\Phi[\dots]$ and with contractions above the operators. This can be accomplished via Wick's theorem (see Eq. 3.25). We only need to know the values of different Wick contractions. For our quasiparticle field operators, we find

$$\overline{b_p b_q^\dagger} = \delta_{pq}, \quad (3.40)$$

$$\overline{b_p b_q} = 0, \quad (3.41)$$

$$\overline{b_p^\dagger b_q^\dagger} = 0, \quad (3.42)$$

$$\overline{b_p^\dagger b_q} = 0, \quad (3.43)$$

exactly the same as for the physical field operators when normal ordering with respect to the physical vacuum.

The case of physical field operators is more relevant to us, since our operators are given in terms of physical creation and annihilation operators. For the physical field operators, we find

$$\overline{a_p a_q^\dagger} = (1 - n_p) \delta_{pq}, \quad (3.44)$$

$$\overline{a_p a_q} = 0, \quad (3.45)$$

$$\overline{a_p^\dagger a_q^\dagger} = 0, \quad (3.46)$$

$$\overline{a_p^\dagger a_q} = n_p \delta_{pq}. \quad (3.47)$$

Assuming we have a Hamiltonian with one-, two-, and three-body operators,

$$H = H^{(1)} + H^{(2)} + H^{(3)}, \quad (3.48)$$

we can normal order it with respect to our reference state by making use of Eq. 3.25 and the contractions above. Doing this yields the following expression for our normal-ordered Hamiltonian:

$$\bar{H}^{(0)} = \sum_i H_{ii}^{(1)} + \frac{1}{2} \sum_{ij} H_{ijij}^{(2)} + \frac{1}{6} \sum_{ijk} H_{ijkijk}^{(3)}, \quad (3.49)$$

$$\bar{H}_{pq}^{(1)} = H_{pq}^{(1)} + \sum_i H_{piqi}^{(2)} + \frac{1}{2} \sum_{ij} H_{pijqij}^{(3)}, \quad (3.50)$$

$$\bar{H}_{pqrs}^{(2)} = H_{pqrs}^{(2)} + \sum_i H_{pqirsi}^{(3)}, \quad (3.51)$$

$$\bar{H}_{pqrstu}^{(3)} = H_{pqrstu}^{(3)}. \quad (3.52)$$

With this we have normal ordered our Hamiltonian with respect to our reference state, obtaining our normal-ordered Hamiltonian. Additionally, we can bring any products of normal-ordered operators to a normal-ordered form by applying the generalized Wick's theorem.

At this point, a few comments are in order about the choice of our reference state $|\Phi\rangle$. The choice of reference state corresponds to a partitioning of our Hamiltonian into a part that is exactly solved by the reference state and a part that contributes corrections to this zeroth-order solution, schematically

$$H = H_0 + H_1, \quad (3.53)$$

as in perturbation theory. A reasonable choice for the reference state corresponds to a choice that solves a problem “approximately” like the problem of interest, for example a spherical harmonic oscillator for spherical bound systems. The normal-ordered zero-body part of the Hamiltonian $\bar{H}^{(0)}$ is the expectation value of the ground-state energy as a result of the partitioning. $\bar{H}^{(1)}$, $\bar{H}^{(2)}$, and $\bar{H}^{(3)}$ do not contribute to this expectation value by construction. To improve the approximation of the physical ground state, one can:

1. improve the reference state, as is discussed in Section 3.3,
2. and/or include corrections to the ground-state wave function, for example admixtures of one-particle one-hole excited states $|\Phi_i^a\rangle$, as is discussed in Section 3.4.

3.3 The Hartree-Fock method

The variational principle states that the true ground state $|\psi\rangle$ globally minimizes the energy functional

$$E[|\psi\rangle] = \frac{\langle\psi|H|\psi\rangle}{\langle\psi|\psi\rangle}. \quad (3.54)$$

However, the ground state will in general not be describable by a single Slater determinant, meaning that cannot hope to get the exact ground-state energy by normal ordering our Hamiltonian with respect to some optimized reference state. Still, one can optimize the reference state within a space restricted to Slater determinants to get the best possible single Slater determinant approximation to the ground state.

This is the core idea behind the Hartree-Fock method [38–40]. Working from a known single-particle basis $|p\rangle$, one wants to find a new single-particle basis $|p'\rangle$ such that our reference state

$$|\Phi\rangle = |p'_1 \dots p'_A\rangle \quad (3.55)$$

has the minimal energy expectation value, or Hartree-Fock energy,

$$\langle\Phi|H|\Phi\rangle = \bar{H}^{(0)}. \quad (3.56)$$

Rewriting the optimized basis in terms of our original basis,

$$|p'\rangle = \sum_{p''} C_{p''p} |p''\rangle, \quad (3.57)$$

where C is a unitary matrix giving the basis transformation, we can expand the Hartree-Fock energy using our Hamiltonian from Eq. 3.48 as

$$\bar{H}^{(0)} = \sum_{i'} H_{i'i'}^{(1)} + \frac{1}{2} \sum_{i'j'} H_{i'j'i'j'}^{(2)} + \frac{1}{6} \sum_{i'j'k'} H_{i'j'k'i'j'k'}^{(3)}, \quad (3.58)$$

where these matrix elements can be connected back to those in our known single-particle basis,

$$H_{i'i'}^{(1)} = \sum_{pq} C_{pi'}^* H_{pq}^{(1)} C_{qi'} , \quad (3.59)$$

$$H_{i'j'i'j'}^{(2)} = \sum_{pqrs} C_{pi'}^* C_{qj'}^* H_{pqrs}^{(2)} C_{ri'} C_{sj'} , \quad (3.60)$$

$$H_{i'j'k'i'j'k'}^{(3)} = \sum_{pqrstu} C_{pi'}^* C_{qj'}^* C_{rk'}^* H_{pqrstu}^{(3)} C_{si'} C_{tj'} C_{uk'} . \quad (3.61)$$

The minimization of $\bar{H}^{(0)}$ gives the Hartree-Fock equations,

$$\sum_q F_{pq} C_{qr} = C_{pr} e_r , \quad (3.62)$$

where F_{pq} is the Fock matrix given by

$$F_{pq} = H_{pq}^{(1)} + \sum_{rsj'} C_{rj'}^* H_{prqs}^{(2)} C_{sj'} + \frac{1}{2} \sum_{rstuj'k'} C_{rj'}^* C_{sk'}^* H_{prsqtu}^{(3)} C_{tj'} C_{uk'} , \quad (3.63)$$

and e_i are Lagrange multipliers ensuring orthonormality of the new single-particle basis. Using that

$$\sum C_{p,i'}^* C_{q,i'} = \rho_{pq} , \quad (3.64)$$

the one-body density in the known single-particle basis, we can simplify Eq. 3.63 to

$$F_{pq} = H_{pq}^{(1)} + \sum_{rs} \rho_{rs} H_{prqs}^{(2)} + \frac{1}{2} \sum_{rstu} \rho_{rt} \rho_{su} H_{prsqtu}^{(3)} . \quad (3.65)$$

These equations are solved self-consistently, where in each iteration k : the density $\rho^{(k-1)}$ of the previous iteration is used to construct the new Fock matrix $F^{(k)}$, $F^{(k)}$ is diagonalized, a new $C^{(k)}$ is constructed from the eigenvectors of $F^{(k)}$, and the density $\rho^{(k)}$ is constructed via Eq. 3.64. To start, we choose $\rho_{pq}^{(0)} = n_p \delta_{pq}$. The iteration terminates when between iterations the $e_i^{(k)}$ change by less than some threshold. At this point, we can transform all operators to our new optimized single-particle basis by applying C appropriately. After this transformation $\bar{H}^{(1)}$ is diagonal with diagonal matrix elements e_i , the single-particle energies.

3.4 Many-body perturbation theory

Many-body perturbation theory (MBPT) has its formal roots in formal perturbation theory, which abstractly gives the perturbation theory formalism. MBPT then specifies certain details about the system and the starting point for perturbation theory and translates the formalism into concrete formulas for order-by-order corrections to the wave function and the energy of a state. In this section we give the key results from formal perturbation

theory, discuss the setup for MBPT, and give the formulas for second- and third-order MBPT corrections to the energy. We refer the interested reader to Refs. [41, 42] for a more comprehensive treatment.

To start, one partitions the Hamiltonian

$$H = H_0 + H_1, \quad (3.66)$$

into H_0 , for which the solution to the Schrödinger equation is known exactly with solutions $|\Phi_k\rangle$ and corresponding energies $E_k^{(0)}$, and a perturbation H_1 . One is interested in an expansion of the true eigenstate $|\Psi_k\rangle$ in terms of the unperturbed solutions $|\Phi_k\rangle$. We concentrate our discussion here on an expansion for the ground state, so the ground state of H is denoted $|\Psi\rangle$ and the ground state of H_0 , the starting point of the expansion, is denoted $|\Phi\rangle$ with an unperturbed energy $E^{(0)}$.

The partitioning comes with the definition of the projection operators

$$P = |\Phi\rangle \langle\Phi|, \quad (3.67)$$

$$Q = \sum_{k \neq 0} |\Phi_k\rangle \langle\Phi_k|. \quad (3.68)$$

Working with the so-called intermediate normalization

$$\langle\Psi|\Phi\rangle = 1, \quad (3.69)$$

one can write the ground state of H as

$$|\Psi\rangle = (P + Q) |\Psi\rangle \quad (3.70)$$

$$= |\Phi\rangle + |\chi\rangle, \quad (3.71)$$

where $|\chi\rangle = Q |\Psi\rangle$ is what needs to be solved for.

The result of formal perturbation theory is that using the Rayleigh-Schrödinger resolvent

$$R = \sum_{k \neq 0} \frac{|\Phi_k\rangle \langle\Phi_k|}{E^{(0)} - E_k^{(0)}} \quad (3.72)$$

the correction to the unperturbed ground state is given by

$$|\chi\rangle = \sum_{n=1}^{\infty} (RH_1)^n |\Phi\rangle_c, \quad (3.73)$$

where the ‘c’ subscript indicates that the expansion is connected, which ensures its size extensivity, that is, that calculated observables scale linearly with the size of the system. The corrections to the energy beyond the standard first-order energy correction

$$E^{(1)} = \langle\Phi|H_1|\Phi\rangle, \quad (3.74)$$

are given by

$$\Delta E = \langle \Phi | H_1 | \chi \rangle \quad (3.75)$$

$$= \langle \Phi | H_1 \sum_{n=1}^{\infty} (RH_1)^n | \Phi \rangle_c . \quad (3.76)$$

As an example, the second-order correction to the energy is

$$E^{(2)} = \sum_{k \neq 0} \frac{\langle \Phi | H_1 | \Phi_k \rangle \langle \Phi_k | H_1 | \Phi \rangle}{E^{(0)} - E_k^{(0)}} . \quad (3.77)$$

This makes it clear that the corrections to the ground state involve the perturbation H_1 connecting the unperturbed ground state in the P -space to excited states in the Q -space before connecting these back to the ground state.

Transitioning to (single-reference) many-body perturbation theory, we define our A -body Hilbert space as comprising our reference state and n -particle n -hole excitations of the reference state:

$$\{ |\Phi\rangle, |\Phi_i^a\rangle, |\Phi_{ij}^{ab}\rangle, |\Phi_{ijk}^{abc}\rangle, \dots \} . \quad (3.78)$$

After normal ordering with respect to $|\Phi\rangle$, we have our normal-ordered zero- through three-body operators, $\bar{H}^{(0)}$, $\bar{H}^{(1)}$, $\bar{H}^{(2)}$, and $\bar{H}^{(3)}$. This choice of basis corresponds to the following partitioning: our unperturbed Hamiltonian is

$$H_0 = \bar{H}^{(0)} + \text{diag}(\bar{H}^{(1)}) \quad (3.79)$$

$$= \bar{H}^{(0)} + \sum_p e_p N_{\Phi} [a_p^\dagger a_p] , \quad (3.80)$$

where $e_p = \bar{H}_{pp}^{(1)}$ are the single-particle energies. The energy of the reference state is given by $\bar{H}^{(0)}$. The energy of an n -particle n -hole excited state $|\Phi_{ij\dots}^{ab\dots}\rangle$ is given by

$$\bar{H}^{(0)} + \epsilon_{ij\dots}^{ab\dots} \quad (3.81)$$

with

$$\epsilon_{ij\dots}^{ab\dots} = (e_a + e_b + \dots) - (e_i + e_j + \dots) . \quad (3.82)$$

The perturbation is then

$$H_1 = \bar{H}^{(1)} - \text{diag}(\bar{H}^{(1)}) + \bar{H}^{(2)} + \bar{H}^{(3)} . \quad (3.83)$$

Finally, the many-body resolvent is

$$R = - \sum_{ai} \frac{|\Phi_i^a\rangle \langle \Phi_i^a|}{\epsilon_i^a} - \frac{1}{(2!)^2} \sum_{abij} \frac{|\Phi_{ij}^{ab}\rangle \langle \Phi_{ij}^{ab}|}{\epsilon_{ij}^{ab}} - \frac{1}{(3!)^2} \sum_{abcijk} \frac{|\Phi_{ijk}^{abc}\rangle \langle \Phi_{ijk}^{abc}|}{\epsilon_{ijk}^{abc}} + \dots . \quad (3.84)$$

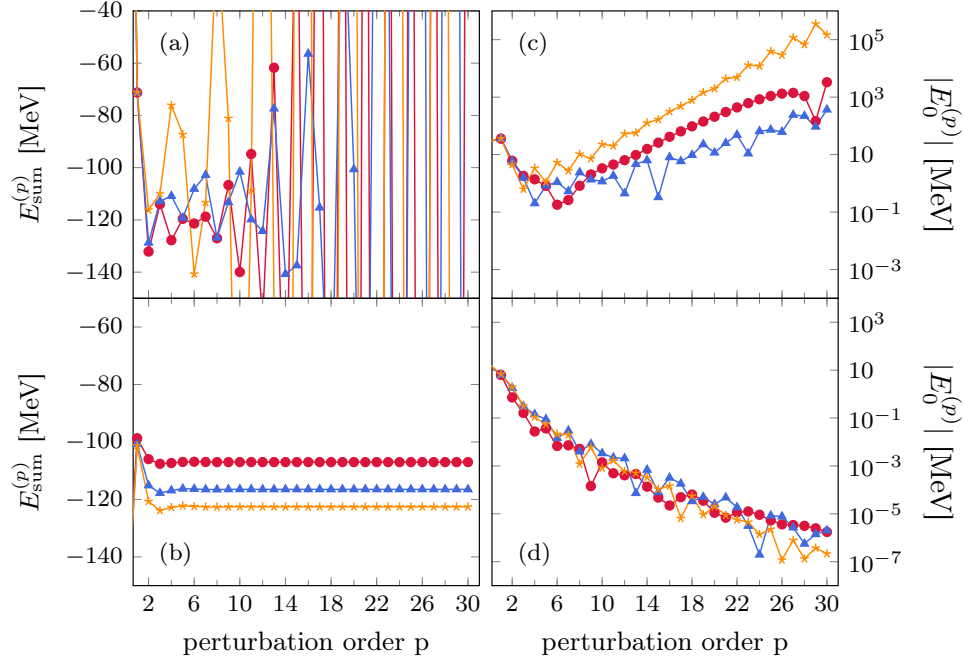


Figure 3.1: The partial sums (left) and order-by-order contributions (right) for an MBPT calculation of the ground-state energy of ^{16}O using a harmonic-oscillator reference state (top) and a Hartree-Fock reference state (bottom). The red, blue, and yellow points are for $N_{\text{max}} = 2, 4$, and 6 , the basis truncation parameter for the approach used. Figure taken from Ref. [43].

We are now in a position to discuss the second- and third-order contributions to the ground-state energy. Using Eq. 3.84 and the properties of normal-ordered operators, the second-order correction to the ground-state energy is given by

$$E^{(2)} = - \sum_{ai} \frac{\bar{H}_{ai}^{(1)} \bar{H}_{ia}^{(1)}}{\epsilon_i^a} - \frac{1}{(2!)^2} \sum_{abij} \frac{\bar{H}_{abij}^{(2)} \bar{H}_{ijab}^{(2)}}{\epsilon_{ij}^{ab}} - \frac{1}{(3!)^2} \sum_{abcijk} \frac{\bar{H}_{abcijk}^{(3)} \bar{H}_{ijkabc}^{(3)}}{\epsilon_{ijk}^{abc}}. \quad (3.85)$$

The first term in this equation is related to a so-called non-canonical diagram that vanishes if we choose the Hartree-Fock (HF) reference state to be our determinant. This is because, as mentioned previously, $\bar{H}^{(1)}$ is by definition diagonal in the HF basis.

At the third order, even considering only canonical diagrams, the number of diagrams possible with two- and three-body operators grows to 17. The complete list of these diagrams can be found in Ref. [44]. The canonical contributions involving only the normal-

ordered two-body Hamiltonian are

$$\begin{aligned}
 E_{2\text{-body only}}^{(3)} = & \frac{1}{8} \sum_{abcdij} \frac{\bar{H}_{ijab}^{(2)} \bar{H}_{abcd}^{(2)} \bar{H}_{cdij}^{(2)}}{\epsilon_{ij}^{ab} \epsilon_{ij}^{cd}} \\
 & + \frac{1}{8} \sum_{abijkl} \frac{\bar{H}_{ijab}^{(2)} \bar{H}_{abkl}^{(2)} \bar{H}_{klji}^{(2)}}{\epsilon_{ij}^{ab} \epsilon_{kl}^{ab}} \\
 & - \sum_{abcijk} \frac{\bar{H}_{ijab}^{(2)} \bar{H}_{kbic}^{(2)} \bar{H}_{ackj}^{(2)}}{\epsilon_{ij}^{ab} \epsilon_{kj}^{ac}}.
 \end{aligned} \tag{3.86}$$

The complete set of non-canonical third-order contributions with only one- and two-body operators is given, among other places, in Ref. [45].

The inclusion of additional terms is not the only challenge when dealing with a non-canonical reference state. Choosing a different reference state than the HF determinant corresponds to choosing a worse partitioning for H , that is, more information is held in the perturbation H_1 , as the the HF determinant is the best possible single Slater determinant approximation to the ground state. This less optimal choice can lead to poor convergence behavior of MBPT [43]. For instance, in Fig. 3.1 the ground-state energy of ^{16}O was calculated using a harmonic-oscillator determinant and a Hartree-Fock determinant for the reference state. While for the HF reference state MBPT converges nicely, for the HO reference state the calculation rapidly begins to diverge when going to higher orders in perturbation theory. Additionally, while MBPT benefits strongly from working with SRG-evolved Hamiltonians, it can have difficulty converging even when using an HF reference state for bare nuclear Hamiltonians that are too “hard” [42].

3.5 Non-perturbative techniques

The convergence challenges of MBPT motivate us to consider non-perturbative many-body methods, which sum to all orders certain types of diagrams to produce a convergent result. Coupled cluster theory and the in-medium similarity renormalization group are two examples of such methods. Their non-perturbative nature makes them less sensitive to the choice of reference state (although convergence speed will be affected by a non-canonical choice of reference state) and better able to deal with “harder” nuclear Hamiltonians. We discuss the IM-SRG in detail in the next chapter. Here, we aim to briefly introduce the coupled cluster many-body approach as it shares many similarities with the IM-SRG.

The ansatz for the coupled cluster (CC) approach is describing the ground state as

$$|\Psi\rangle = \exp(T) |\Phi\rangle, \tag{3.87}$$

where T is the cluster operator, which when applied exponentially to the reference state $|\Phi\rangle$ yields the ground state [46]. T contains in general one- through A -body operators,

$$T = T^{(1)} + T^{(2)} + \dots + T^{(A)}, \tag{3.88}$$

which generate particle-hole excitations of the reference state.

The ground-state energy is then given by

$$E = \langle \Psi | H | \Psi \rangle \quad (3.89)$$

$$= \langle \Phi | \exp(-T) (\bar{H}^{(1)} + \bar{H}^{(2)} + \bar{H}^{(3)}) \exp(T) | \Phi \rangle + \bar{H}^{(0)} \quad (3.90)$$

$$\equiv \langle \Phi | \bar{H} | \Phi \rangle + \bar{H}^{(0)}, \quad (3.91)$$

where we have defined the similarity-transformed Hamiltonian \bar{H} . The task is to solve for matrix elements of the different A -body parts of T such that

$$0 = \langle \Phi_{ijk\dots}^{abc\dots} | \bar{H} | \Phi \rangle \quad (3.92)$$

for all n -particle n -hole excited states of the reference state. These are the coupled cluster equations.

One computes \bar{H} via the Baker-Campbell-Hausdorff expansion,

$$\bar{H} = H_N + [H_N, T] + \frac{1}{2!} [[H_N, T], T] + \dots, \quad (3.93)$$

where $H_N = \bar{H}^{(1)} + \bar{H}^{(2)} + \bar{H}^{(3)}$. This commutator expansion ensures that only connected diagrams in the MBPT expansion are generated, ensuring the size-extensivity of the method. A standard approach in nuclear physics is to truncate T , H_N , and the commutator at the two-body level, giving two coupled cluster equations

$$0 = \langle \Phi_i^a | \bar{H} | \Phi \rangle, \quad (3.94)$$

$$0 = \langle \Phi_{ij}^{ab} | \bar{H} | \Phi \rangle, \quad (3.95)$$

known as CCSD (SD for singles and doubles). Another variant approximately treats the so-called triples and is denoted CCSD(T). In the next chapter, when discussing the IM-SRG, the many similarities of the methods will be quite obvious.

Chapter 4

The in-medium similarity renormalization group

The in-medium similarity renormalization group is a modern *ab initio* many-body method that extends the renormalization group approach of decoupling energy scales to many-body calculations. It is a non-perturbative wave function expansion method, in the same vein as coupled cluster, but it operates on the operators rather than the wave function. It is remarkably flexible, with favorable scaling with system size and the ability to target many different observables, and its invention and development has contributed strongly to the rapid expansion of *ab initio* theoretical calculations of medium-mass nuclei. In this chapter, we introduce the IM-SRG formalism. We then discuss the topics of truncation scheme, generator selection, and approaches to solving the flow equations.

4.1 Basic formalism

As a reminder from Section 2.2, the idea behind the SRG is the construction of a continuous unitary transformation of the Hamiltonian

$$H(s) = U(s) H U^\dagger(s), \quad (4.1)$$

which can be obtained by solving the flow equation

$$\frac{dH(s)}{ds} = [\eta(s), H(s)], \quad (4.2)$$

with the anti-Hermitian generator $\eta(s)$. The solution of this flow equation with vacuum normal-ordered operators, the free-space SRG, is appealing in that the evolved operators are not system specific and can be generally used for many-body calculations of nuclei and nuclear matter. However, the free-space SRG evolution can only be done consistently in the two- and three-body spaces for nuclear systems, leaving out induced higher-body operators.

The idea behind the IM-SRG is to solve Eq. 4.2 in-medium, that is, to normal order with respect to a reference state before solving the flow equations. Starting from a Hamiltonian with a one-, two- and three-body part

$$H = H^{(1)} + H^{(2)} + H^{(3)}, \quad (4.3)$$

our normal-ordered Hamiltonian matrix elements are given by

$$E \equiv \bar{H}^{(0)} = \sum_i H_{ii}^{(1)} + \frac{1}{2} \sum_{ij} H_{ijij}^{(2)} + \frac{1}{6} \sum_{ijk} H_{ijkijk}^{(3)}, \quad (4.4)$$

$$f_{pq} \equiv \bar{H}_{pq}^{(1)} = H_{pq}^{(1)} + \sum_i H_{piqi}^{(2)} + \frac{1}{2} \sum_{ij} H_{pijqij}^{(3)}, \quad (4.5)$$

$$\Gamma_{pqrs} \equiv \bar{H}_{pqrs}^{(2)} = H_{pqrs}^{(2)} + \sum_i H_{pqirsi}^{(3)}, \quad (4.6)$$

$$W_{pqrst} \equiv \bar{H}_{pqrst}^{(3)} = H_{pqrst}^{(3)}, \quad (4.7)$$

where we have introduced the conventional names for zero-, one-, two-, and three-body normal-ordered parts of the Hamiltonian, E , f , Γ , and W , used in the literature. As a reminder, indices p, q, r, \dots run over all single-particle states, indices i, j, k, \dots run over holes, single-particle states occupied in the reference state, and indices a, b, c, \dots run over particles, single-particle states unoccupied in the reference state.

In general, the generator $\eta(s)$ has one- through A -body normal-ordered parts

$$\eta(s) = \sum_{i=1}^A \eta^{(i)}(s). \quad (4.8)$$

For now, we leave $\eta(s)$ unspecified beyond its required anti-Hermiticity, which causes it to not have a zero-body part. We discuss the choice of generator in Section 4.3. Concretely, our initial normal-ordered Hamiltonian is

$$\begin{aligned} H = & E + \sum_{pq} f_{pq} \text{N}_\Phi [a_p^\dagger a_q] \\ & + \frac{1}{(2!)^2} \sum_{pqrs} \Gamma_{pqrs} \text{N}_\Phi [a_p^\dagger a_q^\dagger a_s a_r] \\ & + \frac{1}{(3!)^2} \sum_{pqrst} W_{pqrst} \text{N}_\Phi [a_p^\dagger a_q^\dagger a_r^\dagger a_u a_t a_s], \end{aligned} \quad (4.9)$$

and our generator is

$$\begin{aligned} \eta(s) = & \sum_{pq} \eta_{pq}^{(1)}(s) \text{N}_\Phi [a_p^\dagger a_q] \\ & + \frac{1}{(2!)^2} \sum_{pqrs} \eta_{pqrs}^{(2)}(s) \text{N}_\Phi [a_p^\dagger a_q^\dagger a_s a_r] \\ & + \frac{1}{(3!)^2} \sum_{pqrst} \eta_{pqrst}^{(3)}(s) \text{N}_\Phi [a_p^\dagger a_q^\dagger a_r^\dagger a_u a_t a_s] \\ & + \dots \end{aligned} \quad (4.10)$$

The evaluation of the right-hand side of Eq. 4.2 then reduces to the evaluation of commutators of normal-ordered products,

$$\left[N_{\Phi} \left[a_{p_1}^{\dagger} \dots a_{p_M}^{\dagger} a_{q_M} \dots a_{q_1} \right], N_{\Phi} \left[a_{r_1}^{\dagger} \dots a_{r_N}^{\dagger} a_{s_N} \dots a_{s_1} \right] \right], \quad (4.11)$$

which can be simplified into a sum of normal-ordered operators using the generalized Wick's theorem (see Eq. 3.26). The commutator of an M -body operator $A^{(M)}$ and an N -body operator $B^{(N)}$ will in general have contributions of $|M - N|$ -body operators through $M + N - 1$ -body operators,

$$[A^{(M)}, B^{(N)}] = \sum_{k=|M-N|}^{M+N-1} C^{(k)}. \quad (4.12)$$

The right-hand side can then be broken up into zero- through A -body parts. We then identify the zero-body part of the right-hand side with dE/ds , the one-body part with df_{pq}/ds , and so on. This makes it obvious that even if the initial Hamiltonian and generator contain only up to three-body operators the IM-SRG evolution induces higher-body operators, all the way up to A -body operators after a couple integration steps, resulting in coupled flow equations for the zero- through A -body parts of the Hamiltonian. Note that one must also ensure the antisymmetry of the right-hand sides of the two-, three-, and higher-body flow equations so the matrix elements remain antisymmetric.

The discussion here has been focused on the Hamiltonian, but the IM-SRG can also be used to evolve other operators,

$$\frac{dO}{ds} = [\eta(s), O(s)], \quad (4.13)$$

where O has also been normal ordered with respect to our reference state $|\Phi\rangle$. Since the generator $\eta(s)$ should be the same for the evolution of H and O and the reconstruction of the unitary transformation from the evolved form of H is not possible, H and O must naively be evolved simultaneously. In Section 4.4, we discuss an alternative approach to solving the IM-SRG flow equations that allows for the construction of the unitary transformation, resulting in easy evolution of other operators along with the Hamiltonian.

4.2 Truncation schemes

As is the case with the free-space SRG, it is not feasible to do the full A -body evolution, and the flow equations must be truncated at some B -body level. However, the situation is not quite the same as with the free-space SRG. Because the initial normal ordering shifts information about higher-body operators into lower-body normal-ordered operators and the continuous normal ordering absorbs information about induced higher-body operators into lower-body normal-ordered operators, the truncated IM-SRG flow equations still approximately evolve higher-body operators (in the free-space sense) using only the reduced B -body flow equations. In the following sections, we discuss truncating the IM-SRG

at the two-body and three-body level, yielding the so-called IM-SRG(2) and IM-SRG(3) truncations respectively.

4.2.1 IM-SRG(2)

Truncating the flow equation at the two-body level amounts to assuming

$$H(s) \approx E(s) + f(s) + \Gamma(s), \quad (4.14)$$

$$\eta(s) \approx \eta^{(1)}(s) + \eta^{(2)}(s). \quad (4.15)$$

In this approximation, we are not including the three-body part of the initial Hamiltonian exactly. However, the three-body force *does* contribute as it was used in obtaining the normal-ordered zero-, one-, and two-body parts of the Hamiltonian. This is known as the normal-ordered two-body (NO2B) approximation, which has been quite successful in nuclear many-body applications.

Using the generalized Wick's theorem, which yields the fundamental commutators in Appendix A of Ref. [3], one arrives at the flow equations for the Hamiltonian

$$\begin{aligned} \frac{dE}{ds} &= \sum_{pq} n_p \bar{n}_q (\eta_{pq}^{(1)} f_{qp} - f_{pq} \eta_{qp}^{(1)}) \\ &\quad + \frac{1}{4} \sum_{pqrs} n_p n_q \bar{n}_r \bar{n}_s (\eta_{pqrs}^{(2)} \Gamma_{rspq} - \Gamma_{pqrs} \eta_{rspq}^{(2)}), \end{aligned} \quad (4.16)$$

$$\begin{aligned} \frac{df_{pq}}{ds} &= \sum_r (\eta_{pr}^{(1)} f_{rq} - f_{pr} \eta_{rq}^{(1)}) \\ &\quad + \sum_{rs} (n_r - n_s) (\eta_{rs}^{(1)} \Gamma_{sprq} - f_{rs} \eta_{sprq}^{(2)}) \\ &\quad + \frac{1}{2} \sum_{rst} (\bar{n}_r \bar{n}_s n_t + n_r n_s \bar{n}_t) (\eta_{tprs}^{(2)} \Gamma_{rstq} - \Gamma_{tprs} \eta_{rstq}^{(2)}), \end{aligned} \quad (4.17)$$

$$\begin{aligned} \frac{d\Gamma_{pqrs}}{ds} &= \sum_t (1 - P_{pq}) (\eta_{pt}^{(1)} \Gamma_{tqrs} - f_{pt} \eta_{tqrs}^{(2)}) \\ &\quad - \sum_t (1 - P_{rs}) (\eta_{tr}^{(1)} \Gamma_{pqts} - f_{tr} \eta_{pqts}^{(2)}) \\ &\quad + \frac{1}{2} \sum_{tu} (1 - n_t - n_u) (\eta_{pqtu}^{(2)} \Gamma_{turs} - \Gamma_{pqtu} \eta_{turs}^{(2)}) \\ &\quad + \sum_{tu} (n_t - n_u) (1 - P_{pq}) (1 - P_{rs}) \eta_{tpur}^{(2)} \Gamma_{uqts}, \end{aligned} \quad (4.18)$$

where n_p are the occupation numbers of the reference state, $\bar{n}_p = 1 - n_p$, the s -dependence has been suppressed, and the permutation operator P_{pq} exchanges the indices p and q in the following expression.

Eqs. 4.16-4.18 are solved by integrating from $s = 0$ towards $s \rightarrow \infty$ with the initial conditions $E(0) = E$, $f(0) = f$, and $\Gamma(0) = \Gamma$. Given appropriate decoupling (see

Section 4.3), $E(\infty)$ gives the energy of the state targeted by the reference state, for our applications typically the ground state. The cost of this integration is dominated by the final two terms in Eq. 4.18, which scale like $\mathcal{O}(N^6)$, where N is the size of the single-particle basis for the calculation. Another nice property is that the flow equation, due to being a commutator many-body expansion, generates only connected diagrams and thus ensures size extensivity [3]. This is true for any B -body truncation.

4.2.2 IM-SRG(3)

Truncating at the three-body level allows one to exactly include initial three-body forces. One assumes

$$H(s) \approx E(s) + f(s) + \Gamma(s) + W(s), \quad (4.19)$$

$$\eta(s) \approx \eta^{(1)}(s) + \eta^{(2)}(s) + \eta^{(3)}(s), \quad (4.20)$$

yielding additional terms with commutators of $\eta^{(3)}$ and W with zero- through two-body operators and a commutator between $\eta^{(3)}$ and W . The flow equations are

$$\begin{aligned} \frac{dE}{ds} = & \sum_{pq} n_p \bar{n}_q (\eta_{pq}^{(1)} f_{qp} - f_{pq} \eta_{qp}^{(1)}) \\ & + \frac{1}{4} \sum_{pqrs} n_p n_q \bar{n}_r \bar{n}_s (\eta_{pqrs}^{(2)} \Gamma_{rspq} - \Gamma_{pqrs} \eta_{rspq}^{(2)}) \\ & + \frac{1}{36} \sum_{pqrstu} n_p n_q n_r \bar{n}_s \bar{n}_t \bar{n}_u (\eta_{pqrstu}^{(3)} W_{stupqr} - W_{pqrstu} \eta_{stupqr}^{(3)}), \end{aligned} \quad (4.21)$$

$$\begin{aligned} \frac{df_{pq}}{ds} = & \sum_r (\eta_{pr}^{(1)} f_{rq} - f_{pr} \eta_{rq}^{(1)}) \\ & + \sum_{rs} (n_r - n_s) (\eta_{rs}^{(1)} \Gamma_{sprq} - f_{rs} \eta_{sprq}^{(2)}) \\ & + \frac{1}{2} \sum_{rst} (\bar{n}_r \bar{n}_s n_t + n_r n_s \bar{n}_t) (\eta_{tprs}^{(2)} \Gamma_{rstq} - \Gamma_{tprs} \eta_{rstq}^{(2)}) \\ & - \frac{1}{4} \sum_{rstu} (n_r n_s \bar{n}_t \bar{n}_u - \bar{n}_r \bar{n}_s n_t n_u) (\eta_{turs}^{(2)} W_{rspqtu} - \Gamma_{turs} \eta_{rspqtu}^{(3)}) \\ & + \frac{1}{12} \sum_{rstuv} (n_r n_s \bar{n}_t \bar{n}_u \bar{n}_v + \bar{n}_r \bar{n}_s n_t n_u n_v) (\eta_{rsptuv}^{(3)} W_{tuvrsq} - W_{rsptuv} \eta_{tuvrsq}^{(3)}), \end{aligned} \quad (4.22)$$

$$\begin{aligned}
\frac{d\Gamma_{pqrs}}{ds} = & \sum_t (1 - P_{pq})(\eta_{pt}^{(1)}\Gamma_{tqrs} - f_{pt}\eta_{tqrs}^{(2)}) \\
& - \sum_t (1 - P_{rs})(\eta_{tr}^{(1)}\Gamma_{pqts} - f_{tr}\eta_{pqts}^{(2)}) \\
& + \frac{1}{2} \sum_{tu} (1 - n_t - n_u)(\eta_{pqtu}^{(2)}\Gamma_{turs} - \Gamma_{pqtu}\eta_{turs}^{(2)}) \\
& + \sum_{tu} (n_t - n_u)(1 - P_{pq})(1 - P_{rs})\eta_{tpur}^{(2)}\Gamma_{uqts} \\
& + \sum_{tu} (n_t - n_u)(\eta_{tu}^{(1)}W_{upqtrs} - f_{tu}\eta_{upqtrs}^{(3)}) \\
& - \frac{1}{2} \sum_{tuv} (n_t\bar{n}_u\bar{n}_v + \bar{n}_t n_u n_v)(1 - P_{rs})(\eta_{uvtr}^{(2)}W_{tpquvs} - \Gamma_{uvtr}\eta_{tpquvs}^{(3)}) \\
& + \frac{1}{2} \sum_{tuv} (n_t\bar{n}_u\bar{n}_v + \bar{n}_t n_u n_v)(1 - P_{pq})(\eta_{uvtp}^{(2)}W_{trsuvq} - \Gamma_{uvtp}\eta_{trsuvq}^{(3)}) \\
& + \frac{1}{6} \sum_{tuvw} (n_t\bar{n}_u\bar{n}_v\bar{n}_w - \bar{n}_t n_u n_v n_w)(\eta_{tpquvw}^{(3)}W_{uvwtrs} - W_{tpquvw}\eta_{uvwtrs}^{(3)}) \\
& + \frac{1}{4} \sum_{tuvw} (\bar{n}_t\bar{n}_u n_v n_w - n_t n_u \bar{n}_v \bar{n}_w)(1 - P_{pq})(1 - P_{rs})\eta_{tupvws}^{(3)}W_{vwqtur},
\end{aligned} \tag{4.23}$$

$$\begin{aligned}
\frac{dW_{pqrst}}{ds} = & \sum_v P(p/qr)(\eta_{pv}^{(1)}W_{vqrst} - f_{pv}\eta_{vqrst}^{(3)}) \\
& - \sum_v P(s/tu)(\eta_{vs}^{(1)}W_{pqrvtu} - f_{vs}\eta_{pqrvtu}^{(3)}) \\
& + \sum_v P(pq/r)P(s/tu)(\eta_{pqsv}^{(2)}\Gamma_{vrtu} - \Gamma_{pqsv}\eta_{vrtu}^{(2)}) \\
& + \frac{1}{2} \sum_{vw} (1 - n_v - n_w)P(pq/r)(\eta_{pqvw}^{(2)}W_{vwrstu} - \Gamma_{pqvw}\eta_{vwrstu}^{(3)}) \\
& - \frac{1}{2} \sum_{vw} (1 - n_v - n_w)P(s/tu)(\eta_{vwts}^{(2)}W_{pqrsuv} - \Gamma_{vwts}\eta_{pqrsuv}^{(3)}) \\
& + \frac{1}{6} \sum_{vw} (n_v n_w n_x + \bar{n}_v \bar{n}_w \bar{n}_x)(\eta_{pqrvwx}^{(3)}W_{vwxsu} - W_{pqrvwx}\eta_{vwxsu}^{(3)}) \\
& + \frac{1}{2} \sum_{vw} (n_v n_w \bar{n}_x + \bar{n}_v \bar{n}_w n_x)P(pq/r)P(s/tu) \\
& \quad \times (\eta_{vwrxtu}^{(3)}W_{xpqvws} - \eta_{xqrvwu}^{(3)}W_{pwwstx}),
\end{aligned} \tag{4.24}$$

Here, $P(pq/r) = 1 - P_{pr} - P_{qr}$ and $P(p/qr) = 1 - P_{pq} - P_{pr}$ ensure the antisymmetry of the three-body indices.

It is clear that the final two terms in Eq. 4.24 dominate the cost of the integration, scaling like $\mathcal{O}(N^9)$ in the size of our single-particle basis. In the absence of an initial three-body operator, the third term in Eq. 4.24, the three-body part of the commutator of two two-body operators, induces a three-body operator, which leads to the contribution of all other terms later in the integration.

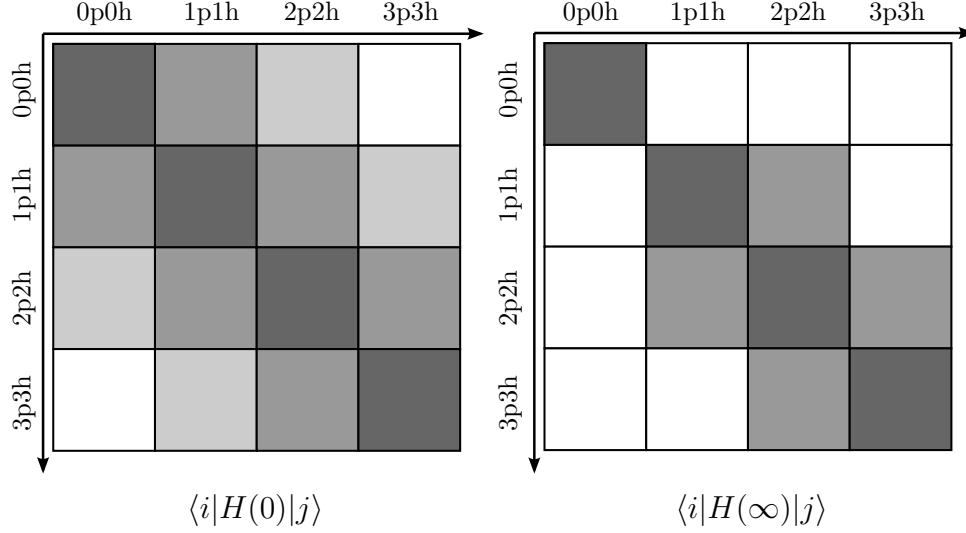


Figure 4.1: Schematic diagram showing the minimal decoupling scheme taken in the IM-SRG. Figure taken from Ref. [3].

We would also like to note that in the derivation of the flow equations here the only assumption that was made was that two- and three-body matrix elements are appropriately antisymmetric. In particular, unlike several other references in the literature, for instance Refs. [3, 9], the flow equations here do not assume f , Γ and W are Hermitian (which of course they are). While this assumption allows for the simplification of certain terms (nothing that changes the scaling of the terms however), it limits the expressions to only commutators of anti-Hermitian and Hermitian operators. In Section 4.4, we require the commutator of two anti-Hermitian operators, for which the right-hand sides of Eqs. 4.16-4.18 and Eqs. 4.21-4.24 are equally valid. For numerical implementations, it is a good idea to implement each of the fundamental commutators separately, to allow for validation and fine-grained optimization in the most expensive commutators.

4.3 Generator selection

So far, we have not discussed specific choices of our generator η . The possible definitions of η hinge on the specification of our so-called “off-diagonal” Hamiltonian H_{od} , the part of the Hamiltonian we wish to suppress to ensure appropriate decoupling in the remaining “diagonal” part. In Section 2.2, we saw that the generator choice $\eta = [T_{\text{rel}}, H(s)]$ leads to the decoupling of any two states with a decay scale set by the difference in their kinetic energy expectation values. The result is that the Hamiltonian evolves towards a diagonal form, providing vastly improved convergence and allowing many-body calculations to use significantly smaller modelspaces.

To identify the desired decoupling for the IM-SRG, we begin by considering the Hamiltonian in the basis spanned by our reference state $|\Phi\rangle$ and n -particle n -hole (nph) excitations of the reference state,

$$\{|\Phi\rangle, |\Phi_i^a\rangle, |\Phi_{ij}^{ab}\rangle, |\Phi_{ijk}^{abc}\rangle, \dots\}. \quad (4.25)$$

For a Hamiltonian with only one- and two-body operators, as is the approximation after normal-ordering for the IM-SRG(2) truncation, the Hamiltonian in this basis is schematically represented in the left panel of Fig. 4.1. It is band-diagonal and only able to couple an nph excitation to $(n \pm 2)p(n \pm 2)h$ excitations. For a Hamiltonian with a three-body part, the band diagonal grows to include $(n \pm 3)p(n \pm 3)h$ excitations.

For the IM-SRG, a decoupling towards a true diagonal form is no longer a good idea, as one must avoid inducing significant three-body terms in the IM-SRG(2) or four- and higher-body terms in the IM-SRG(3) to maintain the validity of the truncation. The alternative is a minimal decoupling scheme, where the sole objective is to decouple the reference state $|\Phi\rangle$ from all nph excitations, as shown in the right panel of Fig. 4.1. Achieving this decoupling gives us the energy of the state E in the zero-body part of the normal-ordered Hamiltonian and the corresponding eigenstate by applying the unitary transformation to the reference state, $U^\dagger(\infty)|\Phi\rangle$. For some finite truncation of the flow equations, this result is of course only approximate.

Now that we know we want to suppress the matrix elements which couple $|\Phi\rangle$ to its excitations, we want to identify which parts of our normal-ordered Hamiltonian these matrix elements correspond to. For the couplings between $|\Phi\rangle$ and $1p1h$ excitations, we find

$$\langle\Phi|H|\Phi_i^a\rangle = \langle\Phi|HN_\Phi[a_a^\dagger a_i]|\Phi\rangle \quad (4.26)$$

$$\begin{aligned} &= E \langle\Phi|N_\Phi[a_a^\dagger a_i]|\Phi\rangle \\ &\quad + \sum_{pq} f_{pq} \langle\Phi|N_\Phi[a_p^\dagger a_q]N_\Phi[a_a^\dagger a_i]|\Phi\rangle \\ &\quad + \sum_{pqrs} \Gamma_{pqrs} \langle\Phi|N_\Phi[a_p^\dagger a_q^\dagger a_s a_r]N_\Phi[a_a^\dagger a_i]|\Phi\rangle \end{aligned} \quad (4.27)$$

$$= \sum_{pq} f_{pq} \delta_{pi} \delta_{qa} n_i \bar{n}_a \quad (4.28)$$

$$= f_{ia}. \quad (4.29)$$

Via similar calculations, one finds

$$\langle \Phi_i^a | H | \Phi \rangle = f_{ai} , \quad (4.30a)$$

$$\langle \Phi | H | \Phi_{ij}^{ab} \rangle = \Gamma_{ijab} , \quad (4.30b)$$

$$\langle \Phi_{ij}^{ab} | H | \Phi \rangle = \Gamma_{abij} , \quad (4.30c)$$

$$\langle \Phi | H | \Phi_{ijk}^{abc} \rangle = W_{ijkabc} , \quad (4.30d)$$

$$\langle \Phi_{ijk}^{abc} | H | \Phi \rangle = W_{abcijk} . \quad (4.30e)$$

We define our “off-diagonal” normal-ordered Hamiltonian then to be

$$\begin{aligned} H_{od} \equiv & \sum_{ia} \left(f_{ia} N_{\Phi} [a_i^{\dagger} a_a] + f_{ai} N_{\Phi} [a_a^{\dagger} a_i] \right) \\ & + \frac{1}{(2!)^2} \sum_{ijab} \left(\Gamma_{ijab} N_{\Phi} [a_i^{\dagger} a_j^{\dagger} a_b a_a] + \Gamma_{abij} N_{\Phi} [a_a^{\dagger} a_b^{\dagger} a_j a_i] \right) \\ & + \frac{1}{(3!)^2} \sum_{ijkabc} \left(W_{ijkabc} N_{\Phi} [a_i^{\dagger} a_j^{\dagger} a_k^{\dagger} a_c a_b a_a] + W_{abcijk} N_{\Phi} [a_a^{\dagger} a_b^{\dagger} a_c^{\dagger} a_k a_j a_i] \right) . \end{aligned} \quad (4.31)$$

We are now in a position where we can define generators that suppress these matrix elements over the course of the flow.

Wegner’s original ansatz for the generator of the SRG flow equation is

$$\eta(s) = [H_d(s), H_{od}(s)] , \quad (4.32)$$

where $H_d = H - H_{od}$ [29]. When using H_{od} as defined above, one can evaluate the commutator truncating at the two- or three-body level depending on the truncation scheme, giving the one-, two-, and three-body components of η in the same form as Eqs. 4.21-4.24. A perturbative analysis of the flow equations with this choice of generator, as is done in Ref. [47], reveals that the two-body “off-diagonal” matrix elements are suppressed like

$$\Gamma_{abij}(s) \approx \Gamma_{abij}(0) \exp(-(\Delta_{abij})^2 s) , \quad (4.33)$$

where Δ_{abij} are the energy denominators. There are multiple options for these energy denominators, corresponding to different partitionings in MBPT (see Section 3.4). We choose to focus on the Møller-Plesset denominators, with $\Delta_{abij} = \epsilon_{abij}$ from Eq. 3.82. Another alternative is the Epstein-Nesbet denominators (see Ref. [41] for details).

We have included the Wegner generator in this discussion for completeness but will not use it in any applications. One reason for this is that the Wegner generator is simply more expensive to construct than the alternatives, which give explicit expressions for the matrix elements of η , resulting in scaling of $\mathcal{O}(N^4)$ and $\mathcal{O}(N^6)$ for IM-SRG(2) and IM-SRG(3), respectively. This is to be contrasted with the evaluation of a full commutator, which scales like $\mathcal{O}(N^6)$ and $\mathcal{O}(N^9)$ for IM-SRG(2) and IM-SRG(3). Additionally, the Wegner generator causes the system of differential equations to be much more stiff, making the

integration much more expensive (in terms of storage and computational requirements) than for other generators.

The following generators directly construct the matrix elements of η , working with a basic form of

$$\begin{aligned} \eta \equiv & \sum_{ia} \left(\eta_{ia}^{(1)} N_{\Phi} [a_i^{\dagger} a_a] + \eta_{ai}^{(1)} N_{\Phi} [a_a^{\dagger} a_i] \right) \\ & + \frac{1}{(2!)^2} \sum_{ijab} \left(\eta_{ijab}^{(2)} N_{\Phi} [a_i^{\dagger} a_j^{\dagger} a_b a_a] + \eta_{abij}^{(2)} N_{\Phi} [a_a^{\dagger} a_b^{\dagger} a_j a_i] \right) \\ & + \frac{1}{(3!)^2} \sum_{ijkabc} \left(\eta_{ijkabc}^{(3)} N_{\Phi} [a_i^{\dagger} a_j^{\dagger} a_k^{\dagger} a_c a_b a_a] + \eta_{abcijk}^{(3)} N_{\Phi} [a_a^{\dagger} a_b^{\dagger} a_c^{\dagger} a_k a_j a_i] \right), \end{aligned} \quad (4.34)$$

where we note that for η to be anti-Hermitian, the matrix elements must fulfill

$$\eta_{ia}^{(1)} = -\eta_{ai}^{(1)}, \quad (4.35a)$$

$$\eta_{ijab}^{(2)} = -\eta_{abij}^{(2)}, \quad (4.35b)$$

$$\eta_{ijkabc}^{(3)} = -\eta_{abcijk}^{(3)}. \quad (4.35c)$$

The White generator corresponds to the choice

$$\eta_{ia}^{(1)}(s) = \frac{f_{ia}(s)}{\Delta_{ia}(s)}, \quad (4.36)$$

$$\eta_{ijab}^{(2)}(s) = \frac{\Gamma_{ijab}(s)}{\Delta_{ijab}(s)}, \quad (4.37)$$

$$\eta_{ijkabc}^{(3)}(s) = \frac{W_{ijkabc}(s)}{\Delta_{ijkabc}(s)}, \quad (4.38)$$

where the antisymmetry of the denominators automatically gives the desired anti-Hermiticity [48]. The White generator suppresses off-diagonal matrix elements like

$$\Gamma_{abij}(s) \approx \Gamma_{abij}(0) \exp(-s), \quad (4.39)$$

that is, it suppresses all off-diagonal matrix elements with the same decay scale, regardless of the energy differences between the states. This is unusual and not strictly speaking in line with the renormalization group approach, where large energy-difference modes are integrated out first. However, we are interested in $H(\infty)$ and $E(\infty)$, and in this limit all generators that suppress H_{od} produce identical results for $E(\infty)$ and $U^{\dagger}(\infty) |\Phi\rangle$, up to truncation effects.

A potential difficulty with the White generator arises when one of the energy denominators becomes very small, leading to large matrix elements of η and thus extremely large derivatives in the right-hand side of the flow equation. This can be mitigated by a

variation of the standard White generator, the arctan generator, with generator matrix elements defined as

$$\eta_{ia}^{(1)}(s) = \frac{1}{2} \arctan \left(\frac{2f_{ia}(s)}{\Delta_{ia}(s)} \right), \quad (4.40)$$

$$\eta_{ijab}^{(2)}(s) = \frac{1}{2} \arctan \left(\frac{2\Gamma_{ijab}(s)}{\Delta_{ijab}(s)} \right), \quad (4.41)$$

$$\eta_{ijkabc}^{(3)}(s) = \frac{1}{2} \arctan \left(\frac{2W_{ijkabc}(s)}{\Delta_{ijkabc}(s)} \right), \quad (4.42)$$

where the arctan function regularizes any possible large matrix elements arising due to small energy denominators.

The final generator we discuss here is the imaginary-time generator, which was ostensibly inspired by imaginary-time evolution techniques in Quantum Monte Carlo methods [3]. Its matrix elements are defined as

$$\eta_{ia}^{(1)}(s) = \text{sign}(\Delta_{ia}(s)) f_{ia}(s), \quad (4.43)$$

$$\eta_{ijab}^{(2)}(s) = \text{sign}(\Delta_{ijab}(s)) \Gamma_{ijab}(s), \quad (4.44)$$

$$\eta_{ijkabc}^{(3)}(s) = \text{sign}(\Delta_{ijkabc}(s)) W_{ijkabc}(s). \quad (4.45)$$

A perturbative analysis of the flow equations with this generator choice shows that off-diagonal matrix elements are suppressed like

$$\Gamma_{abij}(s) \approx \Gamma_{abij}(0) \exp(-|\Delta_{abij}|s). \quad (4.46)$$

The sign function in the definition of the generator ensures that there is an absolute value around the energy denominator in the exponential, giving a suppression for all matrix elements instead of an enhancement for some. We also note here that the imaginary-time generator produces a “proper” RG flow, where matrix elements coupling large energy differences are suppressed before those coupling smaller energy differences.

4.4 The Magnus expansion

Working with Eqs. 4.16-4.18 and 4.21-4.24, one can solve the IM-SRG by numerically integrating the system of ordinary differential equations (ODEs) to obtain the energy and the expectation values of other observables in the targeted state. This approach has two main challenges: First, the flow equations need to be solved to high precision, as otherwise numerical effects destroy the unitarity of the transformation even in the absence of any truncation. This necessitates the application of sophisticated ODE solvers to minimize this numerical error. These solvers require the allocation of several times the memory requirement of two- and three-body operators, which is already quite a lot (on the order of GB or tens of GB), and the evaluation of each integration step is substantially

more expensive (providing the benefit of reduced accumulated numerical error) than an Euler method. This is incidentally also a reason the White, arctan, and imaginary-time generators are preferred over the Wegner generator, as the stiffness of the flow equations with the Wegner generator requires the use of stiff ODE solvers, which are even more expensive in terms of storage and computational cost than their non-stiff counterparts.

Second, the evolution of other operators along with the Hamiltonian requires them to be evolved in parallel in this approach. This means that for every additional operator the memory and computational cost increases by the amount that it would cost to just solve the Hamiltonian. Furthermore, additional operators may increase the stiffness of the system of ODEs as the integration scales for their matrix elements may differ from the Hamiltonian. This challenge can be alleviated by the ability to construct the unitary transformation for the evolution, $U(s)$.

This is the goal of the Magnus expansion approach to solving the IM-SRG flow equations [49]. Given our definition of $\eta(s)$ following Eq. 2.3, we get a differential equation for $U(s)$,

$$\frac{dU(s)}{ds} = -\eta(s)U(s), \quad (4.47)$$

where $U(0) = 1$. The formal integral of this differential equation is

$$U(s) = \mathcal{T}_s \left[\exp\left(-\int_0^s ds' \eta(s')\right) \right], \quad (4.48)$$

where \mathcal{T}_s is the time-ordering operator with respect to s [50].

The Magnus expansion postulates that a solution of the form

$$U(s) = \exp(\Omega(s)) \quad (4.49)$$

exists, where $\Omega(s)$ is anti-Hermitian and $\Omega(0) = 0$ [51]. To obtain $\Omega(s)$, one solves the differential equation of its expansion in $\eta(s)$,

$$\frac{d\Omega(s)}{ds} = \sum_{k=0}^{\infty} \frac{B_k}{k!} ad_{\Omega(s)}^k(\eta(s)), \quad (4.50)$$

where B_k are the Bernoulli numbers and ad_{Ω}^k are the recursively defined commutators,

$$ad_{\Omega(s)}^0(\eta(s)) = \eta(s), \quad (4.51)$$

$$ad_{\Omega(s)}^k(\eta(s)) = [\Omega(s), ad_{\Omega(s)}^{k-1}(\eta(s))]. \quad (4.52)$$

The interested reader may refer to Ref. [52] for detailed review of the Magnus expansion.

Here we note that $ad_{\Omega(s)}^k(\eta(s))$ is anti-Hermitian for all k , thus truncating Eq. 4.50 at any order gives an exactly anti-Hermitian approximation to $d\Omega(s)/ds$, which when integrated gives an exactly anti-Hermitian approximation to $\Omega(s)$. Thus $U(s) = \exp(\Omega(s))$ is always exactly unitary, regardless of accumulated numerical error in the solution for

$\Omega(s)$. This alleviates the requirement of using high-order ODE solvers to avoid numerical error, and the solution of the IM-SRG flow equations in this approach can proceed using a cheap numerical integrator, for example a simple Euler method.

To apply the obtained unitary transformation to our Hamiltonian or some other operator, we use the Baker-Campbell-Hausdorff (BCH) formula,

$$H(s) = e^{\Omega(s)} H(0) e^{-\Omega(s)} = \sum_{k=0}^{\infty} \frac{1}{k!} ad_{\Omega(s)}^k(H(0)). \quad (4.53)$$

To be concrete, the evaluation of the IM-SRG flow equations in the Magnus formalism proceeds as follows:

1. the generator $\eta(s)$ is constructed from $H(s)$,
2. the derivative $d\Omega(s)/ds$ is obtained via Eq. 4.50 and applied via a simple Euler method,
3. the new evolved Hamiltonian $H(s + ds)$ is obtained via Eq. 4.53,

repeating these steps until E is sufficiently converged. For practical calculations, a few truncations must be made. First, $H(s)$, $\eta(s)$, $\Omega(s)$, and all commutators must be truncated at the B -body level, leading to the Magnus(2) and Magnus(3) analogues to the IM-SRG(2) and IM-SRG(3) truncations. Additionally, the Magnus and BCH expansions (Eqs. 4.50 and 4.53) must be truncated at some finite k . For the Magnus expansion, we truncate the series when the norm of the k -th term drops below a threshold ϵ_{deriv} ,

$$\left| \frac{B_k ||ad_{\Omega(s)}^k(\eta(s))||}{k! ||\Omega(s)||} \right| < \epsilon_{\text{deriv}}. \quad (4.54)$$

A similar condition can also be used for the truncation of the BCH expansion, with the threshold ϵ_{BCH} ,

$$\left| \frac{||ad_{\Omega(s)}^k(H(0))||}{k! ||\Omega(s)||} \right| < \epsilon_{\text{BCH}}. \quad (4.55)$$

An alternative, for when one is only interested in the zero-body part of the evolving Hamiltonian, is

$$\left| \frac{ad_{\Omega(s)}^k(H(0))^{(0)}}{k!} \right| < \epsilon_{\text{BCH}}. \quad (4.56)$$

The Magnus expansion makes very clear the similarities and differences between the IM-SRG and coupled cluster. Both use a nested commutator expansion, ensuring the connected nature of the expansion and guaranteeing size extensivity. The IM-SRG and CC seek to generate a similarity transformation that decouples the reference state expectation

value from the rest of the Hamiltonian. However, in coupled cluster the cluster operator T is non-Hermitian, meaning that the BCH expansion for the similarity transformation truncates at a finite order. The IM-SRG generates a unitary transformation, which means Ω , the Magnus analogue of the cluster operator, is anti-Hermitian. This leads to an infinite BCH expansion that must be truncated at some order.

In the next chapter, we present various results for many-body calculations obtained using the IM-SRG. Nearly all of these are done using the Magnus formalism, as its computational benefits are invaluable to doing calculations with three-body operators.

Chapter 5

Results

In this chapter, we discuss the application of the IM-SRG to calculate the ground-state energies of two different fermionic systems. The first is the pairing Hamiltonian, which has been used to study pairing effects in finite and infinite systems. We use this well-studied system as a benchmark for our numerical implementation, as its small modelspace allows for calculations to complete relatively quickly. The second is ${}^4\text{He}$, the lightest closed-shell nucleus, in a restricted modelspace in the IM-SRG(2). The results of our implementation are then compared against those from another open-source IM-SRG(2) library.

5.1 The pairing Hamiltonian

The pairing Hamiltonian is given by

$$H = \delta \sum_{p\sigma} (p-1) a_{p\sigma}^\dagger a_{p\sigma} - \frac{g}{2} \sum_{pq} a_{p+}^\dagger a_{p-}^\dagger a_{q-} a_{q+}, \quad (5.1)$$

where we have equally-spaced two-fold degenerate levels indexed by the quantum number p and an attractive (for $g > 0$) pairing interaction. Cooper first considered this Hamiltonian in 1956 [53], which led to the successful Bardeen-Cooper-Schreifer (BCS) theory of superconductivity [54]. The exact eigenvalues of the pairing Hamiltonian were given by Richardson in 1963, where the solutions are obtained via the solution of the non-linear coupled Richardson equations [55].

We focus on a restricted case where $p = 1, \dots, 4$ and $\delta = 1 \text{ MeV}$, and we vary the strength of the pairing interaction g . We are interested in the ground state of four fermions, for which our reference state is the state with the two lowest levels completely filled,

$$|\Phi\rangle = a_{2-}^\dagger a_{2+}^\dagger a_{1-}^\dagger a_{1+}^\dagger |0\rangle. \quad (5.2)$$

This system has a couple of useful properties: First, the number of single-particle states is only eight, making the IM-SRG(3) calculation relatively tractable. Additionally, one can increase the number of levels p_{max} easily to get a handle on the performance for larger

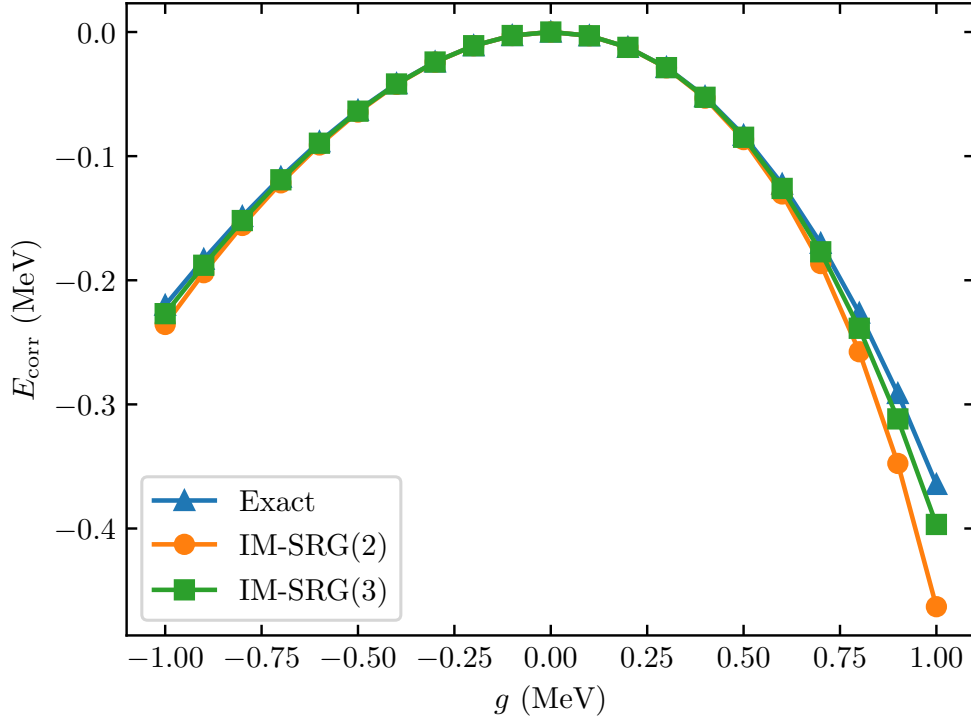


Figure 5.1: The correlation energy E_{corr} for the solution of the pairing Hamiltonian obtained via exact diagonalization, IM-SRG(2), and IM-SRG(3) for $-1 \leq g \leq 1$. Exact diagonalization results obtained using code published with Ref. [56].

single-particle basis sizes. Second, in addition to the available exact solution, this system is easy to construct and diagonalize in the basis of the reference state and its particle-hole excitations,

$$\{|\Phi\rangle, |\Phi_{ij}^{ab}\rangle, |\Phi_{ijkl}^{abcd}\rangle\}, \quad (5.3)$$

where the odd number particle-hole excitations do not contribute as Eq. 5.1 only couples pairs. This makes it easy to obtain an exact solution with which to compare the IM-SRG(2) and IM-SRG(3) solutions. Finally, after normal ordering the Hamiltonian with respect to our reference state, we find that $\bar{H}^{(1)}$ is diagonal, meaning our reference state is the canonical Hartree-Fock reference state with the Hartree-Fock energy $\bar{H}^{(0)} = E_{\text{HF}} = 2 - g$. This means the IM-SRG evolution must only bring in correlation corrections to the energy without needing to overcome any reference state deficiencies.

Thus, we are interested in the correlation energy obtained by the IM-SRG(2) and IM-SRG(3) solutions, defined as

$$E_{\text{corr}} = E(\infty) - E(0). \quad (5.4)$$

This is plotted in Fig. 5.1 for $-1 \leq g \leq 1$. We find generally good agreement between the IM-SRG correlation energy and the exact correlation energy, with the exception of the region for $0.5 \leq g \leq 1$. Here, the IM-SRG(3) calculation improves upon the relatively large error in the IM-SRG(2) correlation energy, which in Ref. [47] was explained as being due to an overcounting in the fourth-order diagrams in MBPT by a factor of 1/2 present in the IM-SRG(2) truncation. It seems that this overcounting at fourth-order is lifted in the IM-SRG(3) replaced by some overcounting at a higher MBPT order, where the contributions are smaller in magnitude. We note here that our results for IM-SRG(2) match exactly with those from Ref. [47].

5.2 ${}^4\text{He}$

The second system we consider here is ${}^4\text{He}$, the lightest closed-shell nucleus. Before we begin a discussion about the details of the system, a few comments are in order. The following calculation is restricted to a very small modelspace, one insufficient to achieve converged results for observables. This is because our implementation does not take advantage of the rotational invariance of spherically symmetric systems, that is, that the normal-ordered two- and three-body Hamiltonians are diagonal in J and \mathcal{J} and independent of M_J and $M_{\mathcal{J}}$. The exploitation of the symmetries leads to so-called J -scheme IM-SRG flow equations. The current results are a benchmark implementation for the IM-SRG(2) that are compared against an existing IM-SRG(2) J -scheme implementation [57]. This serves as an additional validation of our implementation in addition to the results for the pairing Hamiltonian. The current implementation will serve as a benchmark against which we can compare our J -scheme IM-SRG(3) implementation, which will be the focus of the next phase of this project.

As input into our calculation, we start with the intrinsic A -body Hamiltonian with only an initial two-body interaction,

$$H_{\text{int}} = T_{\text{int}} + V^{(2)}, \quad (5.5)$$

with the intrinsic kinetic energy

$$T_{\text{int}} = T - T_{\text{cm}} \quad (5.6)$$

$$= \left(1 - \frac{1}{A}\right) \sum_i \frac{p_i^2}{2m} - \frac{1}{A} \sum_{i < j} \frac{p_i \cdot p_j}{m}. \quad (5.7)$$

We note that the first term gives us our one-body Hamiltonian and the second term contributes to the two-body Hamiltonian along with $V^{(2)}$ [58].

We work in the single-particle harmonic-oscillator basis at several different values of $\hbar\Omega$ (see Section 2.3.3), with the single-particle states

$$|n_a(l_a s_a) j_a m_{j_a} t_a m_{t_a}\rangle \equiv |\alpha_a\rangle, \quad (5.8)$$

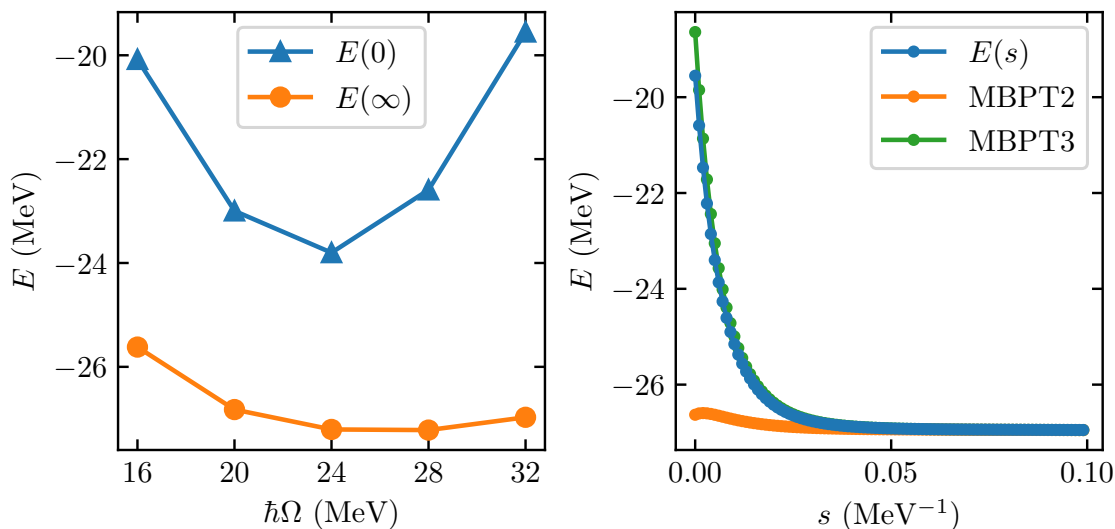


Figure 5.2: The left panel shows $E(0)$ and $E(\infty)$ for an IM-SRG(2) calculation of ${}^4\text{He}$ for $\hbar\Omega$ ranging from 16 MeV to 32 MeV. The interaction used is the EM NN interaction with a regulator cutoff $\Lambda = 500$ MeV and SRG-evolved to $\lambda = 1.8 \text{ fm}^{-1}$ [18]. The right panel shows the flowing energy $E(s)$ along with the energy with second- and third-order MBPT corrections included for $\hbar\Omega = 32$ MeV.

where $s_a = 1/2$ and $t_a = 1/2$. A natural ordering of these states is according to their energy quantum number, $e = 2n + l$. For the following calculation, we truncate the single-particle basis at $e_{\text{max}} = 2$. The resulting size of our single-particle basis is $N = 40$. As our reference state for ${}^4\text{He}$ we choose to fill the four $e = 0$ HO states, the most reasonable choice to target the ground state without solving for and transforming to the Hartree-Fock basis.

For $V^{(2)}$, we use the EM NN potential from Ref. [18] at N3LO with a regulator cutoff at $\Lambda = 500$ MeV and SRG-evolved to $\lambda = 1.8 \text{ fm}^{-1}$. This potential has been shown to reproduce experimental binding energies across the nuclear chart very well [11]. The results from normal ordering our Hamiltonians at the different $\hbar\Omega$ with respect to our HO reference state and evaluating the IM-SRG(2) evolution are shown in the left panel of Fig. 5.2. We find that the unevolved energy $E(0)$, that is, the energy expectation value of the reference state, is already good to within 30% of the exact result, a consequence of the SRG-softened interaction we are using. Still, the IM-SRG evolution absorbs up to 8 MeV of correlation energy into the ground-state energy. We also find that our implementation agrees with the implementation from Ref. [57] to within 10^{-5} MeV.

In the right panel of Fig. 5.2, we show the flowing ground-state energy as well as the ground-state energy with second- and third-order MBPT corrections. We find that these corrections vanish as the correlations are absorbed into the ground-state energy, indicating that we are achieving the desired decoupling. We emphasize once again that these results

are intended to be interpreted as validation (for example, as a nuclear-like toy model) and not as physically meaningful. We consider the agreement between our implementation and that of Ref. [57] to be *a posteriori* evidence of the correctness of our implementation.

Chapter 6

Summary and outlook

In this thesis, we aim to study the ground-state properties of closed-shell nuclear systems in the IM-SRG(3). As a first step in that direction, we have implemented a generic IM-SRG(2)/(3) solver, which we applied at the IM-SRG(2) truncation level to the calculation of the ${}^4\text{He}$ ground-state energy and at the IM-SRG(2) and IM-SRG(3) level to the pairing Hamiltonian. At the IM-SRG(2) level, we found excellent agreement between our implementation and existing IM-SRG(2) implementations and published results [47, 57]. For the pairing Hamiltonian at the IM-SRG(3) level, we found that the three-body truncation does reduce the discrepancy between IM-SRG(2) and the exact solution in the region of large coupling. This can be interpreted as evidence that the many-body expansion is behaving systematically, a claim that we would also like to verify in nuclear systems.

In principle, the next step would be to calculate ${}^4\text{He}$ with the same Hamiltonian in the IM-SRG(3), where one would expect the corrections due to the three-body truncation to be small. With our $e_{\text{max}} = 2$, this amounts to solving a system of approximately 4 billion coupled differential equations, most of which are the flowing matrix elements of the three-body Hamiltonian W . Of course, many of these matrix elements are not independent, related to one another via antisymmetry or (anti-)Hermiticity, and many should be exactly equal to 0, such as those that are blocked by the Pauli exclusion principle. By exploiting these symmetries, it may be possible to allow the current implementation of IM-SRG(3) to also work for ${}^4\text{He}$. This would offer the ability to look at many different metrics, such as the flowing ground-state energy and the MBPT corrections, when implementing a J -scheme IM-SRG(3) library. Even if the performance is insufficient, a calculation can be run for a few integration steps and the implementation of the fundamental commutators can be used to benchmark the J -scheme implementation of the fundamental commutators.

Looking forward to the next phase of the project, some key deliverables will be:

1. implementing a correct J -scheme IM-SRG(3) solver for use in nuclear many-body calculations using automatic recoupling tools [59];

2. tuning the performance of the solver to reach single-particle basis sizes large enough for observables to be reasonably converged;
3. calculating the ground-state energies (and possibly other observables) for ${}^4\text{He}$ and ${}^{16}\text{O}$ in the IM-SRG(3) and systematically studying the effects of the three-body truncation.

It will be interesting to see if the improvement looks significantly different for different Hamiltonians and if there are some well-reasoned physically-motivated ways to approximate the IM-SRG(3) well that could be used to extend current large-scale IM-SRG(2) implementations. Some options for such approximations might be the inclusion of certain terms that dominate the IM-SRG(3) contributions or the development of a way to include sparse approximate three-body operators that provide the dominant IM-SRG(3) contributions. With a robust implementation of our own, we will be in an excellent position to systematically study these options and many more.

Bibliography

- [1] National Research Council. *Nuclear Physics: Exploring the Heart of Matter*. The National Academies Press, Washington, DC, 2013.
- [2] J. Erler, N. Birge, M. Kortelainen, W. Nazarewicz, E. Olsen, A. M. Perhac, and M. Stoitsov. The limits of the nuclear landscape. *Nature*, 486:509–512, 2012.
- [3] H. Hergert, S. K. Bogner, T. D. Morris, A. Schwenk, and K. Tsukiyama. The In-Medium Similarity Renormalization Group: A Novel Ab Initio Method for Nuclei. *Phys. Rept.*, 621:165–222, 2016.
- [4] S. Weinberg. Phenomenological Lagrangians. *Physica A*, 96:327–340, 1979.
- [5] H.-W. Hammer, S. König, and U. van Kolck. Nuclear effective field theory: status and perspectives. *Rev. Mod. Phys.*, 92:025004, 2020.
- [6] K. G. Wilson. Renormalization group and critical phenomena. 1. Renormalization group and the Kadanoff scaling picture. *Phys. Rev. B*, 4:3174–3183, 1971.
- [7] S. K. Bogner, R. J. Furnstahl, and R. J. Perry. Similarity Renormalization Group for Nucleon-Nucleon Interactions. *Phys. Rev. C*, 75:061001, 2007.
- [8] S. K. Bogner, R. J. Furnstahl, and A. Schwenk. From low-momentum interactions to nuclear structure. *Prog. Part. Nucl. Phys.*, 65:94–147, 2010.
- [9] K. Tsukiyama, S. K. Bogner, and A. Schwenk. In-Medium Similarity Renormalization Group for Nuclei. *Phys. Rev. Lett.*, 106:222502, 2011.
- [10] R. B. Wiringa, V. G. J. Stoks, and R. Schiavilla. Accurate nucleon-nucleon potential with charge independence breaking. *Phys. Rev. C*, 51:38, 1995.
- [11] K. Hebeler. Three-Nucleon Forces: Implementation and Applications to Atomic Nuclei and Dense Matter. 2020.
- [12] E. Epelbaum, H.-W. Hammer, and U.-G. Meißner. Modern Theory of Nuclear Forces. *Rev. Mod. Phys.*, 81:1773–1825, 2009.
- [13] R. Machleidt and D. R. Entem. Chiral effective field theory and nuclear forces. *Phys. Rept.*, 503:1–75, 2011.

- [14] H. Pagels. Departures from Chiral Symmetry: A Review. *Phys. Rept.*, 16:219, 1975.
- [15] R. J. Furnstahl, N. Klco, D. R. Phillips, and S. Wesolowski. Quantifying truncation errors in effective field theory. *Phys. Rev. C*, 92:024005, 2015.
- [16] E. Epelbaum, H. Krebs, and U. G. Meißner. Improved chiral nucleon-nucleon potential up to next-to-next-to-next-to-leading order. *Eur. Phys. J.*, A51:53, 2015.
- [17] E. Epelbaum, H. Krebs, and U. G. Meißner. Precision nucleon-nucleon potential at fifth order in the chiral expansion. *Phys. Rev. Lett.*, 115:122301, 2015.
- [18] D. R. Entem and R. Machleidt. Accurate charge dependent nucleon nucleon potential at fourth order of chiral perturbation theory. *Phys. Rev. C*, 68:041001, 2003.
- [19] D. R. Entem, R. Machleidt, and Y. Nosyk. High-quality two-nucleon potentials up to fifth order of the chiral expansion. *Phys. Rev. C*, 96:024004, 2017.
- [20] S. Ishikawa and M. R. Robilotta. Two-pion exchange three-nucleon potential: $O(q^4)$ chiral expansion. *Phys. Rev. C*, 76:014006, 2007.
- [21] V. Bernard, E. Epelbaum, H. Krebs, and U.-G. Meißner. Subleading contributions to the chiral three-nucleon force. I. Long-range terms. *Phys. Rev. C*, 77:064004, 2008.
- [22] V. Bernard, E. Epelbaum, H. Krebs, and U.-G. Meißner. Subleading contributions to the chiral three-nucleon force II: Short-range terms and relativistic corrections. *Phys. Rev. C*, 84:054001, 2011.
- [23] K. Hebeler, H. Krebs, E. Epelbaum, J. Golak, and R. Skibinski. Efficient calculation of chiral three-nucleon forces up to N³LO for ab initio studies. *Phys. Rev. C*, 91:044001, 2015.
- [24] I. Tews, T. Krüger, K. Hebeler, and A. Schwenk. Neutron matter at next-to-next-to-next-to-leading order in chiral effective field theory. *Phys. Rev. Lett.*, 110:032504, 2013.
- [25] S. Schulz. *Four-Nucleon Forces in Ab Initio Nuclear Structure*. PhD thesis, Technische Universität, Darmstadt, February 2018.
- [26] S. R. Beane, P. F. Bedaque, M. J. Savage, and U. van Kolck. Towards a perturbative theory of nuclear forces. *Nucl. Phys.*, A700:377–402, 2002.
- [27] A. Nogga, R. G. E. Timmermans, and U. van Kolck. Renormalization of one-pion exchange and power counting. *Phys. Rev. C*, 72:054006, 2005.
- [28] E. Epelbaum, A. M. Gasparyan, J. Gegelia, and U.-G. Meißner. How (not) to renormalize integral equations with singular potentials in effective field theory. *Eur. Phys. J.*, A54:186, 2018.

- [29] F. Wegner. Flow-equations for Hamiltonians. *Ann. Phys.*, 506:77–91, 1994.
- [30] S. D. Glazek and K. G. Wilson. Renormalization of Hamiltonians. *Phys. Rev. D*, 48:5863–5872, 1993.
- [31] K. Hebeler. Momentum space evolution of chiral three-nucleon forces. *Phys. Rev. C*, 85:021002, 2012.
- [32] E. D. Jurgenson, S. K. Bogner, R. J. Furnstahl, and R. J. Perry. Decoupling in the Similarity Renormalization Group for Nucleon-Nucleon Forces. *Phys. Rev. C*, 78:014003, 2008.
- [33] M. Moshinsky. Transformation brackets for harmonic oscillator functions. *Nucl. Phys.*, 13:104–116, 1959.
- [34] B. Buck and A. C. Merchant. A simple expression for the general oscillator bracket. *Nucl. Phys.*, A600:387–402, 1996.
- [35] J. C. Slater. The Theory of Complex Spectra. *Phys. Rev.*, 34:1293–1322, 1929.
- [36] G. C. Wick. The Evaluation of the Collision Matrix. *Phys. Rev.*, 80:268–272, 1950.
- [37] W. Kutzelnigg and D. Mukherjee. Normal order and extended Wick theorem for a multiconfiguration reference wave function. *J. Chem. Phys.*, 107:432–449, 1997.
- [38] J. C. Slater. The Self Consistent Field and the Structure of Atoms. *Phys. Rev.*, 32:339–348, Sep 1928.
- [39] V. Fock. Näherungsmethode zur Lösung des quantenmechanischen Mehrkörperproblems. *Z. Phys.*, 61:126–148, 1930.
- [40] D. R. Hartree. The Wave Mechanics of an Atom with a Non-Coulomb Central Field. Part II. Some Results and Discussion. *Math. Proc. Cambridge Philos. Soc.*, 24:111–132, 1928.
- [41] I. Shavitt and R. J. Bartlett. *Many-Body Methods in Chemistry and Physics: MBPT and Coupled-Cluster Theory*. Cambridge Molecular Science. Cambridge University Press, 2009.
- [42] A. Tichai, R. Roth, and T. Duguet. Many-body perturbation theories for finite nuclei. *Front. in Phys.*, 8:164, 2020.
- [43] A. Tichai, J. Langhammer, S. Binder, and R. Roth. Hartree–Fock many-body perturbation theory for nuclear ground-states. *Phys. Lett. B*, 756:283–288, 2016.
- [44] B. S. Hu, T. Li, and F. R. Xu. Ab initio Rayleigh-Schrödinger perturbation calculation including three-body force. 2018.

- [45] A. Tichai. *Many-Body Perturbation Theory for Ab Initio Nuclear Structure*. PhD thesis, Technische Universität, Darmstadt, November 2017.
- [46] G. Hagen, T. Papenbrock, M. Hjorth-Jensen, and D. J. Dean. Coupled-cluster computations of atomic nuclei. *Rept. Prog. Phys.*, 77:096302, 2014.
- [47] H. Hergert, S. K. Bogner, J. G. Lietz, T. D. Morris, S. Novario, N. M. Parzuchowski, and F. Yuan. In-Medium Similarity Renormalization Group Approach to the Nuclear Many-Body Problem. *Lect. Notes Phys.*, 936:477–570, 2017.
- [48] S. R. White. Numerical canonical transformation approach to quantum many-body problems. *J. Chem. Phys.*, 117:7472–7482, 2002.
- [49] T. D. Morris, N. M. Parzuchowski, and S. K. Bogner. Magnus expansion and in-medium similarity renormalization group. *Phys. Rev. C*, 92:034331, 2015.
- [50] F. J. Dyson. The Radiation Theories of Tomonaga, Schwinger, and Feynman. *Phys. Rev.*, 75:486–502, Feb 1949.
- [51] W. Magnus. On the exponential solution of differential equations for a linear operator. *Commun. Pure Appl. Math.*, 7:649–673, 1954.
- [52] S. Blanes, F. Casas, J.A. Oteo, and J. Ros. The Magnus expansion and some of its applications. *Phys. Rept.*, 470:151 – 238, 2009.
- [53] L. N. Cooper. Bound electron pairs in a degenerate Fermi gas. *Phys. Rev.*, 104:1189–1190, 1956.
- [54] J. Bardeen, L. N. Cooper, and J. R. Schrieffer. Theory of superconductivity. *Phys. Rev.*, 108:1175–1204, 1957.
- [55] R.W. Richardson. A restricted class of exact eigenstates of the pairing-force Hamiltonian. *Phys. Lett.*, 3:277 – 279, 1963.
- [56] J. Lietz, S. Novario, G. R. Jansen, G. Hagen, and M. Hjorth-Jensen. Computational Nuclear Physics and Post Hartree-Fock Methods. *Lect. Notes Phys.*, 936:293–399, 2017.
- [57] S. R. Stroberg, H. Hergert, J. D. Holt, S. K. Bogner, and A. Schwenk. Ground and excited states of doubly open-shell nuclei from ab initio valence-space Hamiltonians. *Phys. Rev. C*, 93:051301, 2016.
- [58] H. Hergert and R. Roth. Treatment of the Intrinsic Hamiltonian in Particle-Number Nonconserving Theories. *Phys. Lett. B*, 682:27–32, 2009.
- [59] A. Tichai, R. Wirth, J. Ripoché, and T. Duguet. Symmetry reduction of tensor networks in many-body theory I. Automated symbolic evaluation of $SU(2)$ algebra. 2 2020.